Astronomy & Astrophysics manuscript no. messineo
November 1, 2011

© ESO 2011

arXiv:1110.6843v1 [astro-ph.GA] 31 Oct 2011

Near- and Mid-Infrared colors of evolved stars in the Galactic plane. The $Q1$ and $Q2$ parameters.

M. Messineo[1] and K. M. Menten[1] and E. Churchwell[3] and H. Habing[2]

[1] Max-Planck-Institut für Radioastronomie, Auf dem Hügel 69, D-53121 Bonn, Germany
e-mail: `messineo@mpifr-bonn.mpg.de`
[2] Leiden Observatory, PO Box 9513, 2300 RA Leiden, The Netherlands

[3] Department of Astronomy, University of Wisconsin-Madison, 475 N. Charter street, Madison, WI 53706, USA

Received September 15, 1996; accepted March 16, 1997

ABSTRACT

Context. Mass-loss from evolved stars chemically enriches the interstellar medium (ISM). Stellar winds from massive stars and their explosions as supernovae shape the ISM and trigger star formation. Studying evolved stars is fundamental for understanding galaxy formation and evolution, at any redshift.
Aims. We aim to establish a photometric identification and classification scheme for Galactic mass-losing evolved stars (e.g., WR, RSG, and AGB stars) with the goal of identifying new ones, and subsequently to use the sample as tracers of Galactic structure.
Methods. We searched for counterparts of known Galactic WR, LBV, RSG, and O-rich AGB stars in the 2MASS, GLIMPSE, and MSX catalogs, and we analyzed their properties with near- and mid-infrared color-color diagrams.
Results. We used the $Q1$ parameter, which is a measure of the deviation from the interstellar reddening vector in the $J-H$ versus $H-K_s$ diagram, and we defined a new parameter, $Q2$, that is a measure of the deviation from the interstellar reddening vector in the $J-K_s$ versus $K_s-[8.0]$ diagram. The latter plane enables to distinguish between interstellar and circumstellar reddening, and to identify stars with circumstellar envelopes. WR stars and late-type mass-losing stars (AGBs and RSGs) are distributed in two different regions of the $Q1$ versus $K_s-[8.0]$ diagram. A sequence of increasing $[3.6]-[4.5]$ and $[3.6]-[8.0]$ colors with increasing pulsation amplitudes (SRs, Miras, and OH/IR stars) is found. Spectra of Miras and OH/IR stars have stronger water absorption at 3.0 μm than SR stars or most of the RSGs. Masing Miras stars have water, but stronger SiO (~ 4 um) and CO_2 absorption (~ 4.25 μm), as suggested by their $[3.6]-[4.5]$ colors, bluer than those of non masing stars. A fraction of RSGs (22%) have the bluest $[3.6]-[4.5]$ colors, but small $Q2$ values. We propose a new set of photometric criteria to distinguish among IR bright Galactic stars.
Conclusions. The GLIMPSE catalog is a powerful tool for photometric classification of Galactic mass-losing evolved stars. Our new criteria will yield many new RSGs and WRs.

Key words. Stars: mass-loss, dust: extinction, Stars: Wolf-Rayet, Stars: supergiants, Stars: late-type, Galaxy: stellar content

1. Introduction

Evolved stars are intrinsically bright and, when their luminosities can be established, they may serve as distance indicators. Thus, they are ideal tracers of Galactic structure. Moreover, since they lose mass at high rates, they chemically enrich the Galactic interstellar medium (ISM).

Intermediate mass stars (from ~ 2.2 to ~ 8 $M_\odot$) lose mass at high rates when they go trough the Asymptotic Giant Branch phase (AGB stars), and, thereafter, the planetary nebula (PN) phase, before cooling as white dwarfs. Evolved massive stars (> 8 $M_\odot$) go through several short-lived evolutionary phases (blue supergiants, BSGs, luminous blue variables, LBVs, Wolf-Rayet stars, WRs, yellow supergiants, YSGs, and red supergiants, RSGs). Eventually, they explode as supernovae leaving a neutron star or a black-hole. Late-type stars (red giants, AGBs, and RSGs) are the most prolific dust producers in the Universe (Gehrz 1989). The archetype VY CMa has a mass-loss rate of 10^{-4} $M_\odot$ y^{-1} (Harwit et al. 2001). While RSGs may have higher mass-loss, since $\dot{M} \propto L$, luminous red giants and AGB are more numerous and, account for more than 70% of the dust in the interstellar medium. $\dot{M}$ and L are the stellar mass loss rate and luminosity, respectively (e.g. Gehrz 1989). In contrast, the majority of hot massive stars are not associated with dusty envelopes; WRs produce only 5% of the dust (Gehrz 1989). While massive stars are typically found in or near HII regions and well trace galactic spiral arms (Georgelin & Georgelin 1976). AGBs, which are older and dynamically relaxed, may serve as direct tracers of the Galactic gravitational potential (Habing et al. 2006). Kinematics of AGBs have been successfully used to map mass components devoid of gas (e.g, galactic bars Habing et al. 2006; Messineo et al. 2002).

A census and classification of Galactic evolved stars is of primary importance to understand galaxy formation and evolution. AGBs and RSGs are still poorly modeled, and their relative contribution to the integrated light of a galaxy is quite uncertain. Major difficulties arise from our poor understanding of the complex process of mass-loss. Moreover, observational identification of evolved stars is a difficult task. Optical studies cannot penetrate the inner Galactic regions due to interstellar extinction; stellar classification in the near-infrared is more difficult, because intrinsic near-infrared colors of evolved stars span a small range (Koornneef 1983). Spectroscopic observations may solve the ambiguity, but they requires more telescope time than photometry, and are feasible only for a limited number of objects. Photometric variability, mass-loss, interstellar extinction, and poor knowledge on stellar distances hamper the detection and classification even of these brightest stars.

Several near-infrared and mid-infrared surveys of the whole Galactic plane are now (or will soon become) available, e.g. the Two Micron All Sky survey (2MASS) (Cutri et al. 2003), the Deep Near-Infrared Survey (DENIS) (Epchtein et al. 1999; The 2005), the UKIRT Infrared Deep Sky Survey (UKIDSS) (Lucas et al. 2008), the VISTA survey (Minniti et al. 2010), the Midcourse Space Experiment (MSX) (Price et al. 2001), the ISO infrared survey of the Galactic Plane (ISOGAL) (Schuller et al. 2003), and the Galactic Legacy Infrared Mid–Plane Survey Extraordinaire (GLIMPSE) (Benjamin et al. 2003; Churchwell et al. 2009). The combined use of near- and mid-infrared measurements permits detection of evolved mass-losing stars, as demonstrated with ISOGAL and MSX data (e.g. Alard et al. 2001; Messineo et al. 2005). However, the classification of evolved stars using GLIMPSE data is still largely unexplored. Similar studies have been carried out on the Magellanic Clouds (e.g. Bonanos et al. 2010; Buchanan et al. 2006, 2009; Yang & Jiang 2011). However, these studies suffer from small number statistics, and are limited to an environment with low metallicity.

In the Milky Way, we know about 500 RSGs, 350 WR stars (van der Hucht 2001), and a dozen confirmed LBVs (Clark et al. 2005). Several thousands of AGBs have been detected via their maser emission, or photometric pulsation properties (e.g. Alard et al. 2001; Deguchi et al. 2004; Glass et al. 2001; Habing et al. 2006; Messineo et al. 2002; Sevenster 2002, and references therein). These numbers are too small for quantitatively constraining theories of Galactic formation and evolution (e.g. Habing et al. 2006; Vauterin & Dejonghe 1998), and for significantly sampling short-lived evolutionary phases and their contribution to Galactic chemical enrichment. Galactic models predict about 9 million Miras, ∼ 5000 M supergiants, and ∼ 3000 WR stars (e.g. Gehrz 1989).

Stellar classification based on infrared two-color diagrams was successfully established in the late 1980's, based on data from the Infrared Astronomical Satellite Point Source catalogue (the IRAS PSC) (e.g. van der Veen & Habing 1988). The 60μm/25μm versus 25μm/12μm color-color diagram distinguishes between a carbon and an oxygen-rich chemistry-, and shows a sequence of O-rich circumstellar shells with increasing mass-loss rates. Successful selection of mass-losing late-type stars has been made with data from the MSX survey (e.g. Messineo et al. 2004, 2005; Sevenster 2002; Sjouwerman et al. 2009). A dust sequence of O-rich envelopes is seen also with MSX colors (Sevenster 1999; Sjouwerman et al. 2009). MSX mapped the whole Galactic Plane within 5° of latitude (plus the IRAS gaps) in six bands (the $B1$-band is centered at 4.3 μm, the $B2$ band at 4.35 μm, the A-band at 8.28 μm, the C-band at 12.13 μm, the D-band at 14.65 μm, and the E-band at 21.34 μm). The A-band has a sensitivity of 0.1 Jy, and a spatial resolution of 18.3$''$ (Price et al. 2001). We indicate with [A],[C],[D], and [E], the magnitudes in the 4 MSX bands at 8.28 μm, 12.13μm, 14.65μm, and 21.34μm, respectively.

The IRAC camera on board the Spitzer Space Telescope offers a new view of the sky in four filters (bands are centered at 3.6, 4.5, 5.8, and 8.0 μm Fazio et al. 2004), with a spatial resolution 6 times better than MSX, and a better sensitivity. We indicate with [3.6], [4.5], [5.8], and [8.0], the magnitudes in the four GLIMPSE filters. Buchanan et al. (2009) and Bonanos et al. (2010) developed a set of color criteria for classifying luminous 8 μm sources in the Large Magellanic Cloud (LMC). HII regions can be isolated by their much redder K_s-A colors, while measurements in the four IRAC bands distinguish between RSGs, O-rich and C-rich AGBs. Yang & Jiang (2011) revised the pulsation properties of RSGs in the LMC using a comprehensive list of 191 RSGs (Buchanan et al. 2009). Only 24% of RSGs show regular pulsation (Yang & Jiang 2011). The IR selected sub-sample of LMC RSGs appears to have redder $K_s-[8.0]$ colors (likely due to higher mass-loss rates) than the average sample. RSGs are found to have bluer [3.6] – [4.5] colors than other luminous red stars.

So far, little work has been done on Galactic evolved stars based on GLIMPSE data. WRs have an infrared excess, due to free-free emission from dense stellar winds (Cohen et al. 1975). Hadfield et al. (2007) established a successful selection of WRs based on a combination of 2MASS and GLIMPSE colors, which has been recently revised by Mauerhan et al. (2011). WRs can be identified by combining three color-color diagrams, the $J-H$ versus $J-K_s$ diagram, the [3.6] – [8.0] versus [3.6] – [4.5] diagram, and the $K_s-[8.0]$ versus $J-K_s$ diagram (Figs. 1, 3 and 2). Known WRs have [3.6] – [8.0] > 0.5 mag and [3.6] – [4.5] > 0.1 mag, and in the $K_s-[8.0]$ versus $J-K_s$ diagrams are located on a different sequence than normal OB stars; their distribution with redder colors does not follow the reddening vector. Hadfield et al. reported a detection rate of 65% for emission line massive stars, and 7% for WR stars. Mauerhan et al. reached a detection rate of 95% for emission line massive stars, and up to 40% for WR stars using additional constraints based on the K_s versus $J-K_s$ diagram, and X-ray emission.

An overview of near and mid-infrared colors of bright mass-losing stars in the Milky Way is missing, and providing one is the purpose of the present work. In this work, we study near-infrared and mid-infrared color properties of known Galactic evolved stars-, and define salient color-criteria for selecting new bonafide WR stars, RSGs, and AGBs. In Sect. 2, we report on previous analyses of evolved stars, which are based on GLIMPSE data. In Sect. 3, we describe the samples of known evolved stars, on which we base the new color-criteria. In Sect. 4, we describe the assumed interstellar extinction ratios. Color properties are analyzed in Sect. 5, and discussed in Sect. 6.

2. Sample selection

We collected samples of known evolved massive stars (RSGs, WRs, and LBVs) with spectroscopically determined spectral types. The lists of AGBs were compiled on the basis of maser properties and/or photometric variability information (SiO masing stars, OH/IR stars, Miras, and semiregular stars Habing 1996).

Throughout the text we use the terms of late-type stars and early-type stars. These definitions are only based on effective temperatures and not on luminosity classes. AGBs and RSGs are late-type stars, while LBVs and WRs are early-type stars.

For every object, we searched for counterparts in the 2MASS All-Sky Catalog of Point Sources (Cutri et al. 2003), in the third release of DENIS data available at CDS (catalog B/denis) and in the GLIMPSE catalog (Spitzer Science 2009) using a search radius of 2$''$. The II/293 (GLIMPSE) catalog available from CDS merges the three surveys GLIMPSE-I (v2.0), GLIMPSE-II (v2.0), and GLIMPSE-3D; Catalog and Archive records are also merged.

We searched for counterparts in the Version 2.3 of the MSX Point Source Catalog (PSC) (Egan et al. 2003) using a search radius of 5$''$.

Only sources detected in at least one mid-infrared band were retained for further analysis. Only 2MASS sources with good photometry were retained (i.e., with red flags 1, or 2, or 3, and quality flags A, B, C or D). Specific details on each sample are given in the following sub-sections.

2.1. Wolf Rayet stars

Stars with initial masses larger than 40 $M_\odot$ enter the WR phase when their H surface fractional mass abundance falls below 0.3 and their surface temperature is roughly above 20,000 K (e.g. Bressan et al. 1984; Figer et al. 1997). WRs lose mass at high rates ($\sim 10^{-5}$ $M_\odot$ y^{-1}) with their strong ionized winds, in which free-free emission is produced. This emission can be detected as an infrared excess long-ward of 2 μm (Cohen et al. 1975). Their spectral energy distribution can be described by a central star plus an infrared excess, well described by a power law with a spectral index, α, of -0.6, which corresponds to the predicted index for a free-free emission generated in stellar winds (Felli & Panagia 1981; Wright & Barlow 1975).

WC stars show circumstellar dust, that their dust is likely due to interactions in multiple systems (Waters 2010).

We searched for GLIMPSE and MSX counterparts of a sample of 345 Galactic WR stars (Mauerhan et al. 2011; Messineo et al. 2011, 2009; Shara et al. 2011; van der Hucht 2001). Coordinates by Mauerhan et al. and Messineo et al. are from 2MASS, while those from Shara et al. are from the The Naval Observatory Merged Astrometric Dataset (NOMAD) (Zacharias et al. 2004). The positions of WR stars listed by van der Hucht (2001) are from astrometric catalogs (e.g. Hipparcos), but for a few stars less accurate positions are given. Initially, we searched for possible associations within 10″; a few matches larger than 2″ were individually checked, and coordinates updated by using the spectroscopic catalog by Skiff (2010). The GLIMPSE and 2MASS astrometries agree within 1″.

We retained the 120 GLIMPSE matches within 2″, and the 70 MSX matches within 5″. The low number of GLIMPSE matches is mainly due to the survey coverage (longitude $l < 65°$ and latitude $b < 1°$). 195 out of 345 WRs are located in the range ($|l| < 65°$ and $|b| < 1°$). 22 WRs stars have both MSX and GLIMPSE 8 μm measurements; the mean value of their ($[8.0]-[A]$) color is +0.22 mag with a standard deviation of 0.5 mag. Discrepant measurements, more than 2.5 sigma, are found for WR 125 and WR 93. Both sources are colliding wind binaries of the same type (WC7 + O9) (Norci et al. 2002). For the dusty WR125 WR, variable mid-infrared flux has been reported by Williams et al. (1994).

2.2. Luminous blue variables

LBVs are rare massive stars in transition toward the Wolf-Rayet phase (e.g. Clark et al. 2005; Conti et al. 1995; Martins et al. 2007; Nota et al. 1995; Smith et al. 2004). They are characterized by cyclic photometric variations with amplitudes of 1–2 mag and yearly timescales, at nearly constant bolometric luminosity. Giant eruptions with changes in visual brightness by more than 3 mag may also occur. LBVs have high mass-loss rates; the archetypical LBV, η Car, has a mass-loss rate of $\sim 10^{-4}$ $M_\odot$ yr^{-1} (e.g. Abraham et al. 2005).

LBVs may be surrounded by extended dusty nebulae, which show a variety of morphology and composition. Amorphous and cristalline silicate, forsterite, as well as iron grains, have been observed (Lamers et al. 2001; Peeters et al. 2002; Umana et al. 2010; Waters 2010). PAH emission are found to dominate the [8.0]−band emission of two LBVs (e.g. Pasquali et al. 2002; Peeters et al. 2002; Umana et al. 2010).

We considered a list of 42 confirmed or candidate LBVs in the Milky Way (Clark et al. 2005; Gvaramadze et al. 2010; Mauerhan et al. 2010; Messineo et al. 2011, 2009). We found 18 counterparts in the GLIMPSE catalog and 25 in the MSX catalog. Five stars have 8 μm measurements in both the MSX and GLIMPSE surveys. However, MSX measurements of WR102ka were discarded because of high crowding in the galactic center region (Barniske et al. 2008; Homeier et al. 2003). For the remaining four sources, the mean value of their $[8.0]-[A]$ color is +0.15 mag, with a standard deviation of +0.19 mag.

2.3. Red supergiant stars

RSG stars are late-type stars of initial masses between 8 and 40 $M_\odot$, burning He in their core (e.g. Levesque et al. 2005). RSGs have luminosities log(L/$L_\odot$) from 4 to 5.3, often show irregular photometric variability, and are surrounded by dusty circumstellar envelopes. Their mass-loss rates range from $\sim 10^{-7}$ to $\sim 10^{-4} M_\odot$ yr^{-1} (e.g. Josselin et al. 2000; Verhoelst et al. 2009).

Over 1000 stars are listed as RSGs in the spectroscopic catalog compiled by Skiff (2010). However, several measurements are from the early 1900s, and need to be confirmed. A significant number of RSG stars were recently discovered as members of young massive clusters (e.g. 2MASS and GLIMPSE Messineo et al. 2009). Five young massive stellar clusters (RSGC1, RSGC2, RSGC3, RSGC4, and RSGC5), extraordinarily rich in RSGs (14, 26, > 8, > 9, 7), have been located between 25° and 30° of longitude, at a distance of about 6 kpc probably at the near end-side of the Galactic Bar (Clark et al. 2009; Davies et al. 2007; Figer et al. 2006; Negueruela et al. 2011, 2010). We restricted our analysis to a sample of 119 spectroscopically confirmed RSGs in clusters, because their association with a cluster confirms the luminosity class (Bernabei & Polcaro 2001; Caron et al. 2003; Clark et al. 2009; Davies et al. 2009a, 2008; Eggenberger et al. 2002; Figer et al. 2006, 1999; Mengel & Tacconi-Garman 2007; Mermilliod et al. 2008; Messineo et al. 2011, 2010; Negueruela et al. 2011, 2010; Pierce et al. 2000; Skiff 2010). When comparing the distribution in colors of the 119 RSG stars in clusters with all RSGs listed by Skiff et al., however, no significant differences are seen.

Verhoelst et al. (2009) studied the dust properties of O-rich RSGs envelopes and found a dust condensation sequence resembling that of AGBs (Kemper et al. 2001; Speck et al. 2000; Sylvester et al. 1999). Stars with low mass-loss rates are rich of oxides and alumina, while high mass-loss stars show olivine, and crystalline silicates (Waters 2010). Metallic Fe or amorphous carbon could also be present (Verhoelst et al. 2009; Waters 2010). Buchanan et al. (2009) report PAH emission at 6.2 μm in some LMC RSGs. PAHs are not detected in mid-infrared spectra of Galactic RSG stars obtained with ISO-SWS (Sloan et al. 2003).

Among our sample of 119 RSGs, 69 matches were found with GLIMPSE counterparts and 79 with MSX sources. 34 stars were detected by both the MSX and the GLIMPSE surveys. The mean value of their $[8.0]-[A]$ color is +0.11 mag with a standard deviation of 0.20 mag.

2.4. Mass-losing AGB stars

AGBs are stars with masses below 8 $M_\odot$, with a degenerate core consisting of C and O, and two burning shells. The inner shell is burning He, while the external one is burning H. The presence of two different sources of nuclear energy determines an interplay between these two shells, causing thermal pulses with inward and outward motion of matter. Carbon can be brought onto the stellar surface, and the AGB star is called a C-star, when the ratio of C over O is above 1. The relative numbers of O and C-rich AGBs strongly depend on metallicity. We only consider here O-rich AGBs, since AGBs in the inner Galaxy are mostly O-rich types (Sevenster 1999).

Several different names are used to indicate specific subclasses of AGBs, based on their pulsation properties and/or circumstellar properties (pulsators, masing stars). A detailed review on AGB stars is presented by Habing & Olofsson (2003). Miras are classically defined as AGBs with visual amplitudes larger than 2.5 mag; their periods typically range from 150 to 1500 days. SRs are regular pulsators with visual amplitudes smaller that 2.5 mag; their periods range from 35 to 250 days. AGBs may have circumstellar envelopes, where maser emission originates. AGBs may be called SiO masing stars, or OH/IR stars, if they have SiO or OH maser emission.

Mass-loss in AGBs is caused by stellar pulsation, and increases going from SR stars to Miras and to OH/IR stars, i.e. with increasing periods. It scales with stellar luminosity ($\dot{M} \propto L^{2.7}$ in SRs) and may range from $\sim 10^{-8}$ to $\sim 10^{-3}$ $M_{\odot}$ yr^{-1} (e.g. Alard et al. 2001; Habing & Olofsson 2003; Ortiz et al. 2002). SR stars have typical mass-loss rates from $\sim 10^{-8}$ to $\sim 10^{-6}$ $M_{\odot}$ yr^{-1}, while Miras have mass-loss rates from $\sim 10^{-7}$ to $\sim 10^{-4}$ $M_{\odot}$ yr^{-1}. A median mass-loss rate of 3×10^{-5} $M_{\odot}$ yr^{-1} was estimated for a sample of OH/IR stars in the Galactic center region (Habing & Olofsson 2003, and references therein).

In order to analyze the full range of near- and mid-infrared colors of AGBs, we collected samples of AGBs with known pulsational properties. About 300 SR stars were detected in the MACHO and ISOGAL surveys (Alard et al. 2001; Alcock et al. 1999; Schuller et al. 2003). We found 66 matches with GLIMPSE point sources and 17 with MSX point sources. The 9 sources with available ($[8.0] - [A]$) colors yield a mean color of 0.45 mag with a standard deviation of 0.33 mag.

A sample of 409 large amplitude variables (LAV) was detected in the central 24×24 arcmin^2 of the Galaxy in K-band by Glass et al. (2001). LAVs correspond to optical Miras, with periods from 150d to 800d. We found 291 counterparts to the 409 LAVs in the GLIMPSE catalog and 95 in the MSX catalog. For the 71 LAVs with measurements at ~ 8 μm from both MSX and GLIMPSE surveys, the mean $[8.0] - [A]$ value is 0.24 mag with a standard deviation of 0.8 mag. SiO maser was detected in 77 of these LAVs (54 with a GLIMPSE counterpart and 40 with an MSX counterpart, Imai et al. 2002).

The sample of SiO masing stars of Messineo et al. (2002) consists of 271 stars, which were color selected from the DENIS, ISOGAL, 2MASS and MSX catalogs. Information on variability and photometric properties suggests that the whole sample consists of Mira-like stars (Messineo et al. 2004). This is a sample of mostly AGB stars, but may likely includes a few RSGs (Messineo 2004). Positions have an accuracy of $1''$ (Messineo et al. 2004). For the SiO masing stars, we found 177 GLIMPSE and 258 MSX counterparts. The 125 sources with both 8μm measurements have a mean ($[8.0] - [A]$) =0.34 mag and a standard deviation of 0.42 mag.

Along the text we will consider as an SiO maser sample the SiO masing stars by Messineo et al. (2002) plus the 77 masing LAVs by Glass et al. (2001); Imai et al. (2002), while we will refer to the remaining LAVs by Glass et al. (2001) simply as LAVs. Maser and color properties are discussed in Verheyen et al. (2011).

OH/IR stars are large amplitude AGBs with periods generally longer than 600d (even exceeding 1500 days), and denser circumstellar envelopes than Miras or SRs. The sample of 766 OH/IR stars by Sevenster (2002) consists of two sets of maser stars detected with the VLA and ATCA interferometers ($|l| < 45°$ and $|b| < 3.5°$). Positional uncertainties are typically $1''$. We found 295 GLIMPSE counterparts and 610 MSX counterparts. 90 OH/IR stars were detected at 8μm by both MSX and GLIMPSE. The mean ($[8.0] - [A]$) is 0.35 mag with a standard deviation of 0.52 mag.

The different numbers of matches found in the GLIMPSE and MSX catalogs are due to difference in their sensitivity and sky coverage. While MSX covers the whole Galactic plane to ±5° of latitude, the GLIMPSE survey is confined to a narrow latitude range ±1°. OH/IR stars are bright at 8μm; many were not included in the GLIMPSE catalog, because of saturation. The MSX detection limit in A-band is 100 mJy ($[A] = 6.9$ mag), while the Spitzer/IRAC 8μm channel saturates at 444 mJy ($[A] = 5.3$ mag), and has a 5 sigma detection limit at 2mJy ([8]=11.2 mag).

3. Interstellar extinction

We adopt a near-infrared extinction power law ($A_{\rm K} \propto \lambda^{-\alpha}$) (Fritz et al. 2011; Indebetouw et al. 2005; Messineo et al. 2005; Nishiyama et al. 2006; Rieke et al. 1985; Stead & Hoare 2009), with an index of $\alpha = -1.9$ (Messineo et al. 2005). This index provides consistent measurements of extinction in the $K_{\rm s}$ versus ($J{-}K_{\rm s}$) and $K_{\rm s}$ versus ($H{-}K_{\rm s}$) diagram, also in fields with very high extinction $A_{\rm K_s}> 2$ mag. Furthermore, this index is consistent with that measured with hydrogen recombination lines by Landini et al. (1984). A recent historical review of index measurements is presented by Fritz et al. (2011).

For the GLIMPSE measurements, we used the color excess ratios $E_{\lambda - Ks}/E_{J-Ks}$ calculated by Indebetouw et al. (2005), and we re-calculated the extinction ratios using Eqn. 1 in Indebetouw et al. (2005), and A_J/A_{Ks} from Messineo et al. (2005). The assumed and resulting quantities are listed in Table 1. They are lower than those first reported by Indebetouw et al. (2005). Lower values are also measured toward the Galactic center (Fritz et al. 2011).

The use of slightly different extinction ratios does not affect our analysis, because the average excess colors are much larger than the uncertainties due to interstellar extinction.

4. Color-color diagrams

In order to identify photometric criteria that might separate early-type stars from late-type stars and identify specific types of stars (e.g. WRs and RSGs), we analyzed the distribution of evolved stars in several color-color diagrams.

4.1. $H{-}K_{\rm s}$ versus $J - H$ diagram

Because of their different temperatures, "normal" late-type stars and early-type stars form two parallel sequences with increasing interstellar extinction in the $H{-}K_{\rm s}$ versus $J - H$ diagram. This diagnostic tool is suited to only classify the bulk of a stellar population; it relies on the assumption that mass-losing objects are rare. Mass-loss changes the stellar energy distribution.

Dust grains in the circumstellar envelopes of late-type stars absorb the stellar light and re-emit at longer wavelengths

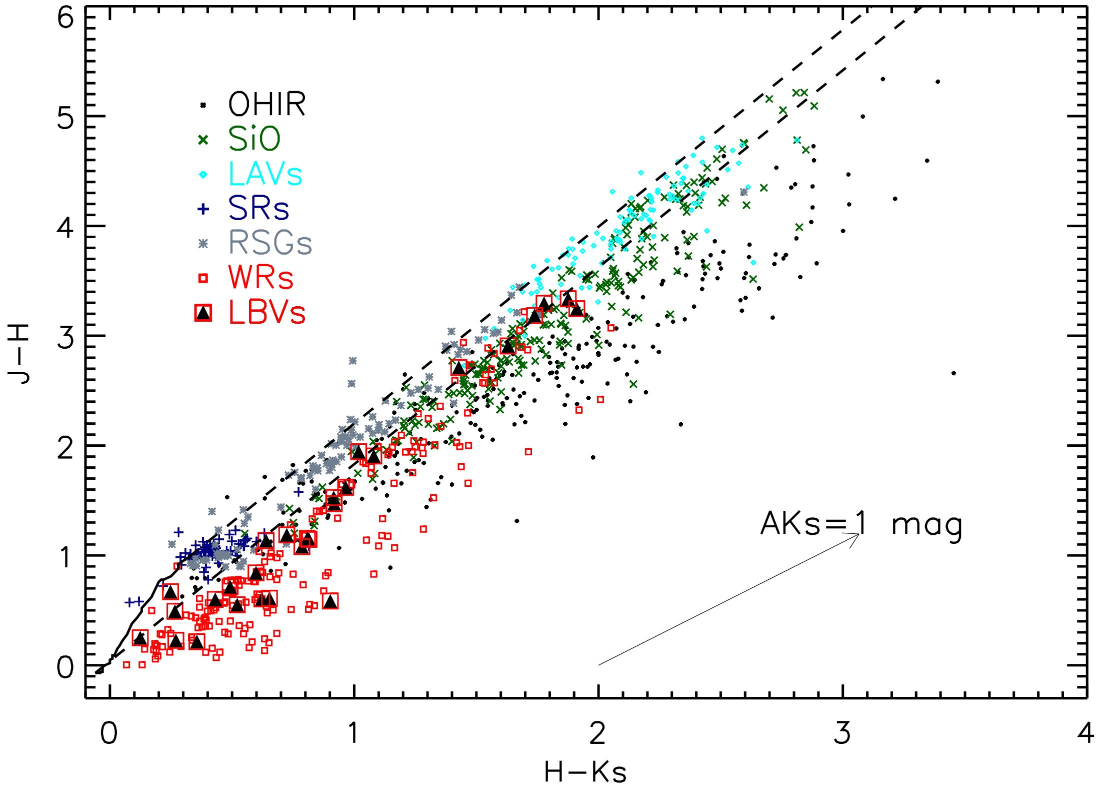

Fig. 1. 2MASS $J-H$ vs. $H-K_s$ diagram of Galactic evolved stars. This diagram does not allow for a photometric classification. SR variables are taken from Alard et al. (2001), large amplitude variables (LAVs) stars from Glass et al. (2001), and AGBs with SiO maser emission from Messineo et al. (2002). OH/IR stars are from Sevenster (2002). The selection of RSGs is described into the text. WR stars are from Messineo et al. (2011, 2009); van der Hucht (2001), LBVs are from Clark et al. (2005); Gvaramadze et al. (2010); Mauerhan et al. (2010, 2011); Messineo et al. (2011). The continuous line near the bottom left corner is the locus of dwarf stars (Koornneef 1983), two dashed lines mark the traces of an O9 (lower) and an M5 (upper) star with increasing interstellar extinction. A reddening vector for A_{K_s}=1 mag is also shown (Messineo et al. 2005). Typical errors are within 0.05 mag in both axis.

Table 1. Infrared extinction ratios (A$_{[\lambda]}$/A_{K_s}) for the 2MASS and SPITZER/IRAC filters.

A_J/A_{Ks}	A_H/A_{Ks}	$A_{[3.6]}/A_{Ks}$	$A_{[4.5]}/A_{Ks}$	$A_{[5.8]}/A_{Ks}$	$A_{[8.0]}/A_{Ks}$	Reference
2.86	1.66					Messineo et al. (2005)
2.5	1.56					Rieke et al. (1985)
2.5 ± 0.2	1.55 ± 0.1	0.56 ± 0.06	0.43 ± 0.08	0.43 ± 0.10	0.43 ± 0.10	Indebetouw et al. (2005)
2.86	1.66	0.44	0.31	0.29	0.31	Indebetouw et al. (2005) and Messineo et al. (2005)

(e.g. Groenewegen & de Jong 1993). In the solar neighborhood, AGBs with low mass-loss rates < 10^{-7} $M_\odot$ yr^{-1} have dereddened $J-K_s$ colors, $(J-K)_o$, between 1.2 and 1.6 mag, while AGB with mass-loss from $10^{-6}-10^{-4}$ have $(J-K)_o$ from 2 to 6.5 mag (Messineo et al. 2005, and references therein). AGBs can have up to 40 mag of visual extinction. Figure 1 shows the $H-K_s$ versus $J-H$ diagram of our samples of evolved stars. Two continuous lines are plotted, showing the loci of a ”naked” M5 star (left/higher dashed line) and of an O9 star (right/lower line) (Koornneef 1983) with varying interstellar extinction, as well as the reddening vector (Messineo et al. 2005). It is not possible to classify stars with this diagram alone, e.g. all Miras would be selected as OB stars. RSGs, SRs, and Galactic center LAV stars appear located between these two lines. SiO and OH/IR stars show even redder $H-K_s$ colors, which are due to continuum absorption in H-band by water (e.g., Fig. 6 and 7 in Blum et al. 2003; Comerón et al. 2004; Frogel & Whitford 1987; Messineo et al. 2005).

WRs seem to define a sequence in Fig. 1, which lies below the sequence of ”normal” OB stars ($H-K_s$ from 0.0 to 1.5 mag and $J-K_s$ from 0.0 to 2.0 mag). The distribution of WRs overlaps that of evolved late-type stars (OH/IR and SiO masing stars). Different physical mechanisms can generate similar $H-K_s$ and $J-H$ colors; LBVs have $J-K_s$ colors from ∼ 1.0 to ∼ 5.0 mag, and $H-K_s$ from ∼ 0.2 mag to ∼ 2.0 mag. A sample of five LBVs (AFGL2298, Pistol Star, WR102ka, LBV1806−20, G0.120−0.048, FMM362) have redder $J-K_s$, which are consistent with distant sources at large interstellar extinction (A_{K_s}=3.15, 2.99, 2.78, 3.0, 3.26, 3.42 mag, respectively Barniske et al. 2008; Bibby et al. 2008; Clark et al. 2003; Mauerhan et al. 2010).

Since circumstellar absorption moves the stars on the diagram almost along the direction of the interstellar reddening vector, it is impossible to distinguish between circumstellar and interstellar reddening with this diagram. An estimate of total (interstellar plus circumstellar) extinction can be obtained from the

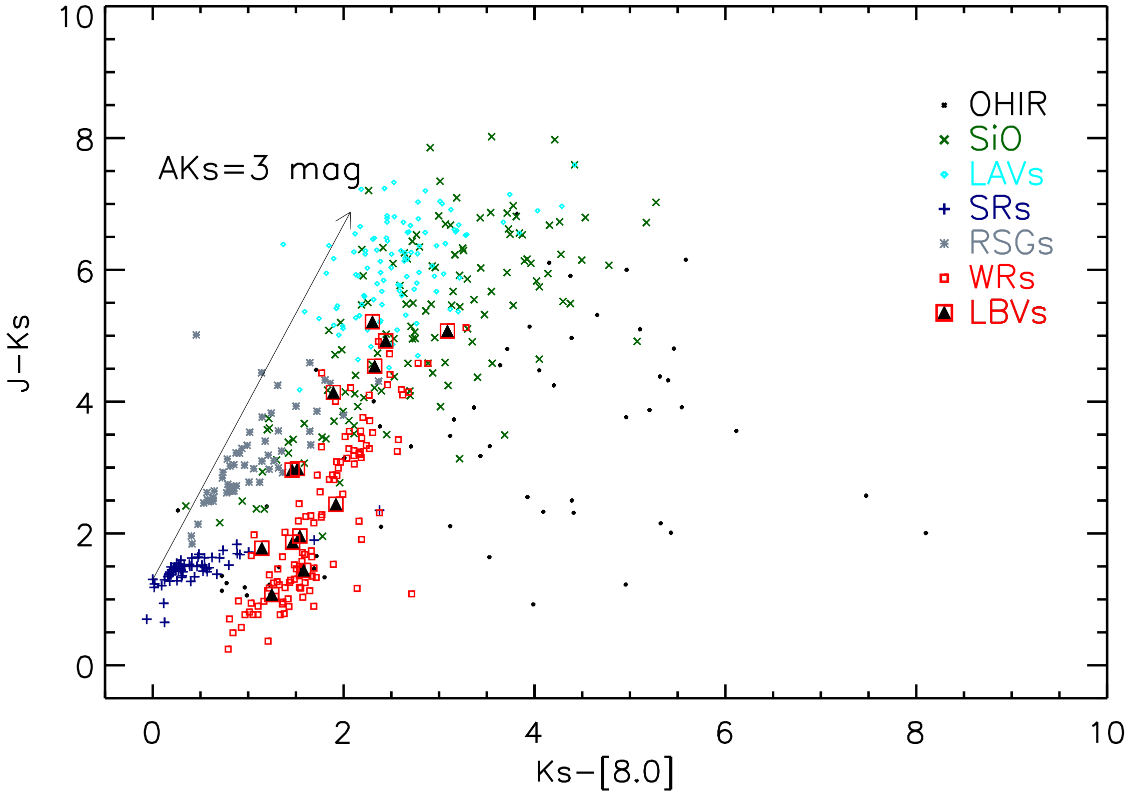

Fig. 2. 2MASS/GLIMPSE K_s–[8.0] versus J–K_s diagram. Symbols are as in Fig. 1. The arrow represents the reddening vector following the extinction ratios given by Messineo et al. (2005) and Indebetouw et al. (2005). Typical errors are within 0.07 mag in both axis.

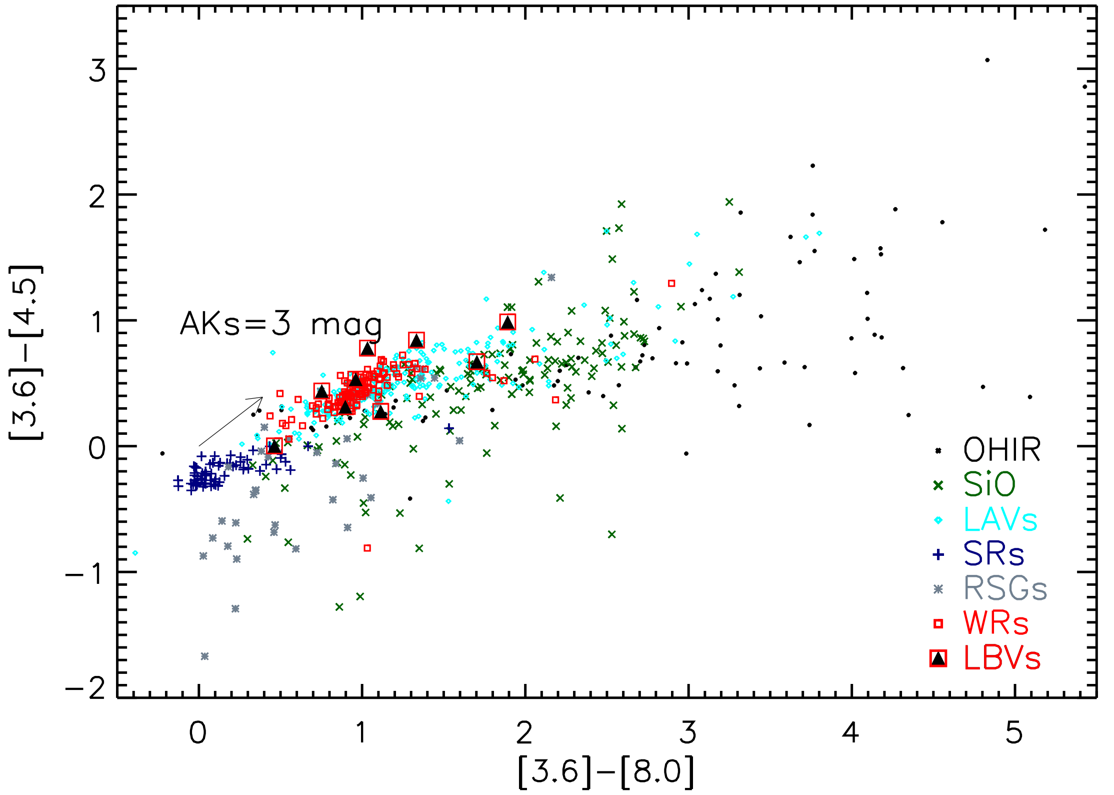

Fig. 3. GLIMPSE [3.6] – [8.0] versus [3.6] – [4.5] diagram. Symbols are as in Fig. 1. The arrow indicates the direction of the reddening vector following the extinction ratios derived by Indebetouw et al. (2005). Typical errors are within 0.08 mag in both axis.

reddening in $J-K_s$, $A_{K_{J-Ks}} = E((J-K_s)) * 0.54$ (Messineo et al. 2005).

4.2. $K_s-[8.0]$ versus $J-K_s$ diagram

A useful diagnostic for mass-loss is a K_s-X versus $J-K_s$ diagram, where X is a mid-infrared magnitude, e.g. the 15 μm measurements made by ISOGAL, or the 8 μm measurements made by MSX and GLIMPSE (e.g. Messineo et al. 2005; van Loon et al. 2003). In Fig. 2, we show a $K_s-[8.0]$ versus $J-K_s$ diagram. The reddening vector is determined using the near-infrared extinction law by Messineo et al. (2005), and the color excess by Indebetouw et al. (2005) (see Sect. 4). A separation between interstellar and circumstellar extinction is detected in this diagram, since increasing circumstellar reddening do not move the star along the direction of the interstellar reddening vector. Deviations from the reddening vector provide evidence for mass-loss (e.g. Messineo et al. 2005, and references therein).

SRs are almost located on the reddening vector, while OH/IR stars show large $K_s-[8.0]$ color excesses (up to 8.0 mag). There is a large overlap between the colors of AGBs (OH/IR stars, SiO masing stars, and Miras) and RSGs stars.

WRs follow a separate sequence in the $K_s-[8.0]$ versus $J-K_s$ diagram (Hadfield et al. 2007). This WR sequence suffers contamination from late-type stars.

4.3. [3.6] – [8.0] versus [3.6] – [4.5] diagram

In Fig. 3, we show a [3.6] – [8.0] versus [3.6] – [4.5] diagram of evolved stars. The reddening vector from Indebetouw et al. (2005) is also marked. Evolved stars do not follow the interstellar reddening vector, but, for a given [3.6] – [4.5] color, they display redder [3.6] – [8.0] colors. We expect interstellar extinction in the IRAC bands below 0.39 mag even in the central regions of the Milky Way ($A_K\sim$ 3 mag) (Indebetouw et al. 2005). Since the ranges of colors seen in Fig. 3 are much larger than this value, we can extract indication on intrinsic colors for each stellar type.

In Fig. 3, AGBs (SRs, Miras, and masing stars) form a sequence of increasing [3.6] – [8.0] colors, from 0.0 (SRs) to 5.0 mag (OH/IR stars). This is likely due to a combination of increasing mass-loss rates and water absorption. SR and LAVs stars display increasing [3.6] – [4.5] colors, with increasing [3.6]−[8.0] colors, likely due to increasing strengths of water absorption at $\sim 3\mu$m. SiO masing stars display peculiar [3.6]−[4.5] colors, bluer than those of SRs and LAVs (without SiO masers). A possible cause is a difference in the water strengths and possible SiO absorption at $\sim$ 4 μm and CO_2 absorption at $\sim$ 4.3 μm(Cami 2002). The distribution of RSGs resembles that of masing AGB stars in this plane. Some RSGs have the bluest [3.6] – [4.5] colors than any other stellar type, as already noted in the LMC, likely due to CO (e.g. Yang & Jiang 2011).

Few ISO-SWS spectra of late-type stars (Sloan et al. 2003) are shown in Appendix.

The bulk of WR stars have [3.6] – [8.0] from 0.5 to 1.5 mag and [3.6] – [4.5] from 0.0 to 0.7 mag. The colors of early type stars, WRs and LBVs, overlap with those of late type stars.

5. The $Q1$ and $Q2$ parameters

5.1. The $Q1$ parameter

The $Q1$ parameter, $Q1 = (J - H) - 1.8 \times (H-K_s)$, is a measure of the deviation from the reddening vector in the $H-K_s$ versus $J-K_s$ plane, following the infrared extinction law by Messineo et al. (2005). This quantity does not depend on interstellar extinction. The $Q1$ parameter was first introduced to photometrically select counterparts of high-mass X-ray binaries (Negueruela & Schurch 2007); it has been successfully used for searching clusters of RSGs (e.g. Clark et al. 2009; Davies et al. 2007; Figer et al. 2006; Negueruela et al. 2011, 2010). Since stars with different spectral types have different intrinsic colors, they will also have a different value of $Q1$, as shown in Table 2 with intrinsic colors by Koornneef (1983). $Q1$ is typically around zero for "normal" OB stars, while it is around 0.4 mag for K-giant stars (Koornneef 1983).

Table 2. $Q1$ values for normal stars (without mass-loss).

Sp. type	I	$Q1$	III	$Q1$	V	$Q1$
O9	I	−0.02	III		V	−0.1
A0	I	0.07	III		V	0.01
F0	I	0.13	III		V	0.13
G3	I	0.31	III	0.36	V	0.23
K0	I	0.36	III	0.41	V	0.29
M5	I	0.72	III	0.68	V	0.38

Table 3. Typical $Q1$ and $Q2$ ranges for the considered sample of stars.

Type	$Q1$ (min)	$Q1$ (max)	$Q2$ (min)	$Q2$ (max)
RSG	−0.06	0.44	−3.38	1.12
WR	−1.19	0.11	−5.02	−1.02
LBV	−0.34	0.06	−2.23	−0.73
OH/IR	−1.56	0.44	−12.99	−0.49
SIO	−0.60	0.30	−7.31	0.69
LAV	−0.17	0.53	−3.01	1.49
SR	0.02	0.52	−1.04	1.46

An infrared excess due to free-free emission in the winds of hot stars (e.g. WRs), or to dusty circumstellar envelopes (e.g. AGBs or RSGs), can modify the $Q1$ parameter of stars. Mass-losing late-type stars may have negative $Q1$ values (similar to those of early type stars). The $Q1$ parameter alone does not allow distinguishing between early and late-type stars.

In Fig. 4, the $Q1$ parameter is plotted against the $K_s-[8.0]$ color. Two panels are shown to separately plot the $Q1$ versus the $K_s-[8.0]$ colors from the 2MASS and GLIMPSE catalogs, and the $Q1$ versus K_s-A colors from the 2MASS and MSX catalogs. The numbers of stars per type are different in the two panels. Most of the OH/IR stars are detected by MSX, but are saturated in GLIMPSE. Galactic center SRs could only be detected with the more sensitive GLIMPSE survey. Typically, $Q1$ is less than 0.1 mag for windy early-type stars, and ranges from −0.1 to 0.4 mag for the bulk of known RSG stars. AGB SRs and AGB LAVs have similar ranges of $Q1$ values, which are also similar to those of RSGs. AGBs with SiO or OH maser emission have broader $Q1$ ranges, OH/IR stars have values down to ~ -1.6 mag (see Table 3). Late-type stars move to redder $K_s-[8.0]$ with decreasing $Q1$ values. Most of the WRs have negative $Q1$ values. LBVs have $Q1$ values range from 0.1 to −0.35 mag.

In Fig. 4 the $Q1$ values are interstellar extinction independent, while the $K_s-[8.0]$ and K_s-A values are affected by interstellar reddening (E($K_s-[8.0]$)), and, therefore, interstellar reddening can only move a data point on a horizontal line. We detected a diagonal cut-off in the distribution of $Q1$ versus $K_s-[8.0]$ values of late-type stars in Fig. 4. This is unrelated to

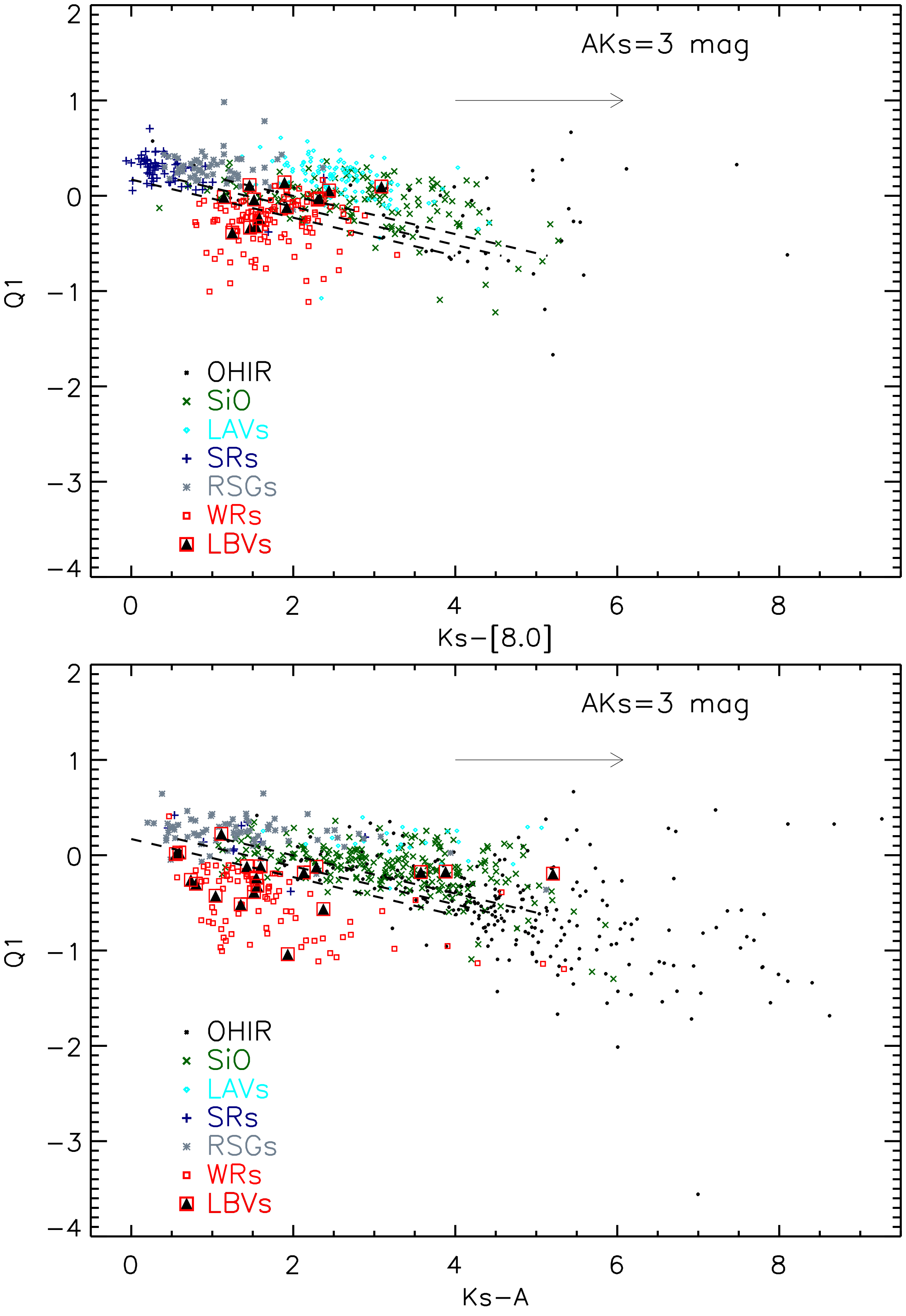

Fig. 4. $Q1$ parameter versus K_s−[8.0]. Symbols are as in Fig. 1. In the top panel the GLIMPSE 8 μm measurements are plotted, while in the bottom panel the MSX 8 μm measurements (A-band) are plotted. The arrow represents the reddening vector following the extinction ratios given by Messineo et al. (2005) and Indebetouw et al. (2005). The dashed lines are a linear fit to the $Q1$ versus the dereddened (K_s−[8.0]) values of SiO masing stars (Messineo 2004) for A_K=0,1,2 mag (from bottom to top). Typical errors are 0.05 mag in the x-axis and 0.14 mag in the y-axis.

interstellar extinction, and arises from the intrinsic stellar energy distribution (SED) of late type stars. The stellar energy distribution significantly changes with increasing mass-loss also in the J, H, and K_s bands. Bolometric corrections in K_s-band (BC_{K_s})

and in A-band ($BC_{\rm A}$) as a function of $K_{\rm s}-A$ were calculated for a sample of SiO masing stars in the inner Galaxy, and compared with those of AGBs in the solar neighbours (Chapter5, Appendix A2 of Messineo 2004; Olivier et al. 2001; Whitelock & Feast 1994; Whitelock et al. 2000, 2003). $BC_{\rm K_S}$ decreases with increasing $K_{\rm s}-A$, and for $K_{\rm s}-A$=6 mag $BC_{\rm K_S}$= 0.8 mag, i.e. $\sim$ 2.3 mag smaller than values for "naked" M-type stars (2.9−3.1 mag) (e.g. Blum et al. 2003; Frogel & Whitford 1987).

We obtained the following relations between the $Q1$ and $K_{\rm s}-[8.0]$ values of SiO masing Mira-like stars (Messineo 2004):

$Q1 = 0.50(\pm0.17) - 0.22(\pm0.05) \times BC_A$

$Q1 = 0.34(\pm0.05) - 0.20(\pm0.04) \times (K_S - A)_o$. where $K_{\rm s}-A$ ranges from $\sim$ 0 to $\sim$ 4 mag.

These relations prove that changes in the SEDs cause variations in the $Q1$ values, and generate the cut-off seen in Fig. 4. Reddening in $K_{\rm s}-A$, due to interstellar extinction, and stellar pulsation smooth such a cut-off by smearing it over $K_{\rm s}-A$ =$\sim$ 1.5 mag. For an $A_{\rm K_s}$ of 1, 2, and 3 mag, E($K_{\rm s}-[8.0]$) =$\sim$ 0.31, $\sim$ 0.62, and $\sim$ 0.93 mag, respectively. This relation nicely explains the diagonal cut-off observed in Fig. 4. OH/IR stars with much redder colors ($K_{\rm s}-A$ > 4.0 mag) may fall below the relation found for SiO masing stars.

This relation between $Q1$ values and $K_{\rm s}-[8.0]$ colors allows a separation of mass-losing late-type stars from hot windy stars (e.g. WR stars). A full revision of bolometric corrections in several near and mid-infrared bands will be the topic of a forthcoming paper.

A few peculiar WRs fall above these lines; WR 125 has a $Q1$ value 0.8 mag above this line when using its MSX 8 μm measurement. This source is known to be dusty and variable (Williams et al. 1994). LBVs cannot be identified in this diagram. Their $(K_S - A)_o$ colors expand over the region of WR stars, as well as over that of late-type stars.

5.2. The $Q2$ parameter

We define a new parameter $Q2 = (J-K_{\rm s}) - 2.69\times(K_{\rm s}-[8.0])$, which is a measure of the deviation from the reddening vector in the $(J-K_{\rm s})$ versus $K_{\rm s}-[8.0]$ plane, following the infrared extinction law of Messineo et al. (2005) and mid-infrared color excess ratios by Indebetouw et al. (2005). $Q2$ can be thought of as a measure of an excess that is only due to a circumstellar shell ($E(K_{\rm s}-[8.0])_{shell}$), and is independent of interstellar extinction: $Q2 \propto (E(K_{\rm s}-[8.0])_{shell})$.

We prefer to use the excess in the $(J-K_{\rm s})$ versus $(K_{\rm s}-[8.0])$, rather than in the $(H-K_{\rm s})$ versus $(K_{\rm s}-[8.0])$ plane, because AGBs may have strong absorption in H-band by gaseous water (see Fig. 1, or Blum et al. 2003; Frogel & Whitford 1987; Messineo et al. 2005).

The $Q2$ parameter can be used to statistically select stars with infrared excess. Such excess can be due to dust emission (late type stars), or free-free emission in shocked winds (WRs); for LBVs it is generally due to free-free emission plus dust emission.

In Fig. 5, the $Q2$ parameter is plotted against the [3.6] − [4.5] color. $Q2$ is a parameter independent of interstellar extinction, interstellar reddening in the [3.6] − [4.5] color are small because the extinction ratios $A_{[3.6]}/A_{\rm K_s}$=0.44 and $A_{[4.5]}/A_{\rm K_s}$=0.31 are similar (Indebetouw et al. 2005). The reddening in [3.6] − [4.5] is 0.13, 0.26, and 0.39 mag, for $A_{\rm K_s}$=1, 2, 3 mag, respectively.

The samples of masing stars (which are mostly Mira-like stars) show typical $Q2$ values from ~ -13 mag to $\sim$ 0.7 mag, but mostly smaller than −1.0 mag. SR stars and RSGs have mostly $Q2$ between 1.5 and −1.1 mag. By combining color and magnitude information it is possible to select bonafide candidate RSG stars, since about 70% of the stars in the range of $Q2$ from −1.1 and 1.5 mag, and [3.6] − [4.5] < −0.4 mag, are RSGs. WR stars have $Q2$ values from −5.0 mag to −1.0. LBVs have a narrow range of $Q2$ values from −2.2 to −0.7 mag.

5.3. $Q1$ versus $Q2$

In Fig. 6 we plot the $Q1$ versus $Q2$ values for the samples of known evolved stars described in Sect. 3. We estimated the $Q1$ and $Q2$ ranges of Table 3 by making histograms of their values and retaining only bins with at least 4 elements; the enclosed fractions are generally above 90%.

Early type stars (with the exception of LBVs) and late type stars are distributed differently in the $Q1$ versus $Q2$ diagram. Early-type stars are mostly located above the relation $Q2 = 11.25 * Q1 - 2.38$ mag, while mass-losing late-types (with the exception of SRs) are mostly located below it. However, a clearer separation between early and late-type stars appears in the $Q1$ vs $K - A$ diagram (see Fig. 4), where early and late-type mass-losing stars can be separated with a 20% error (see Table 4). Specific searches can be optimized by adopting more stringent constraints on $Q1$ and $Q2$, and by using luminosity information.

AGBs form a sequence of decreasing $Q1$ and $Q2$ values going from SRs to OH/IR stars. The bulk of SRs have $Q1$ from 0.0 to +0.5 mag, and $Q2$ from −1.0 to 1.5 mag. LAV stars have similar $Q1$ values, but their $Q2$ values have a larger range (from −3.0 to 1.5 mag). Masing stars have a slightly larger range of $Q1$, from −1.6 mag to 0.4 mag, and generally negative $Q2$, down to −13.0 mag.

The $Q1$ and $Q2$ values of RSGs are similar to those of LAV stars. Their $Q1$ values range from −0.0 to 0.4 mag, and $Q2$ are mostly from −3.4 to 1.1 mag. A large fraction (56 %) of the RSGs appear concentrated in the region $0.1 < Q1 < 0.5$ mag and $-1.1 < Q2 < 1.5$ mag, and 26 % in the narrower region $0.1 < Q1 < 0.5$ mag and $0.5 < Q2 < 1.5$ mag. The fraction of LAVs and masing stars falling in the latter region is below 2%. SR stars cannot be distinguished from RSGs on the basis of colors only (49% of SRs fall into the narrow region). Since SRs are intrinsically much fainter, the degeneracy can be eliminated with luminosity information.

WR stars have distinct $Q1$ and $Q2$ values; typical $Q1$ values are smaller than $\sim$ 0.1 mag and $Q2$ values smaller than −1.0 mag. LBVs have typical $Q1$ values from −0.3 to 0.0 mag, and $Q2$ values from −2.2 to −0.7 mag. A distinct group of three LBVs (Wra751/IRAS11065-6026, AFGL2298, and HD168625) appears at $Q1 \sim -0.2$ mag and $Q2 \sim -9.0$ mag. HD 168625 and AFGL2298 have large $Q2$ values because of their strong PAH emission lines (Pasquali et al. 2002; Peeters et al. 2002; Umana et al. 2010). This suggests that the spectrum of Wra751/IRAS11065-6026 is also dominated by strong PAHs.

6. Suggested selection criteria

There is overlap among the various samples in the color-color diagrams shown in Figs. 1, 2, and 3. It is not possible to uniquely define a photometric classification scheme that is only based on these diagrams. Furthermore, each color depends on interstellar extinction.

We propose a new classification based on two extinction free parameters, $Q1$ and $Q2$ (see Figs. 4, 5, and 6), in which we identify color-windows mostly populated by RSG stars and massive

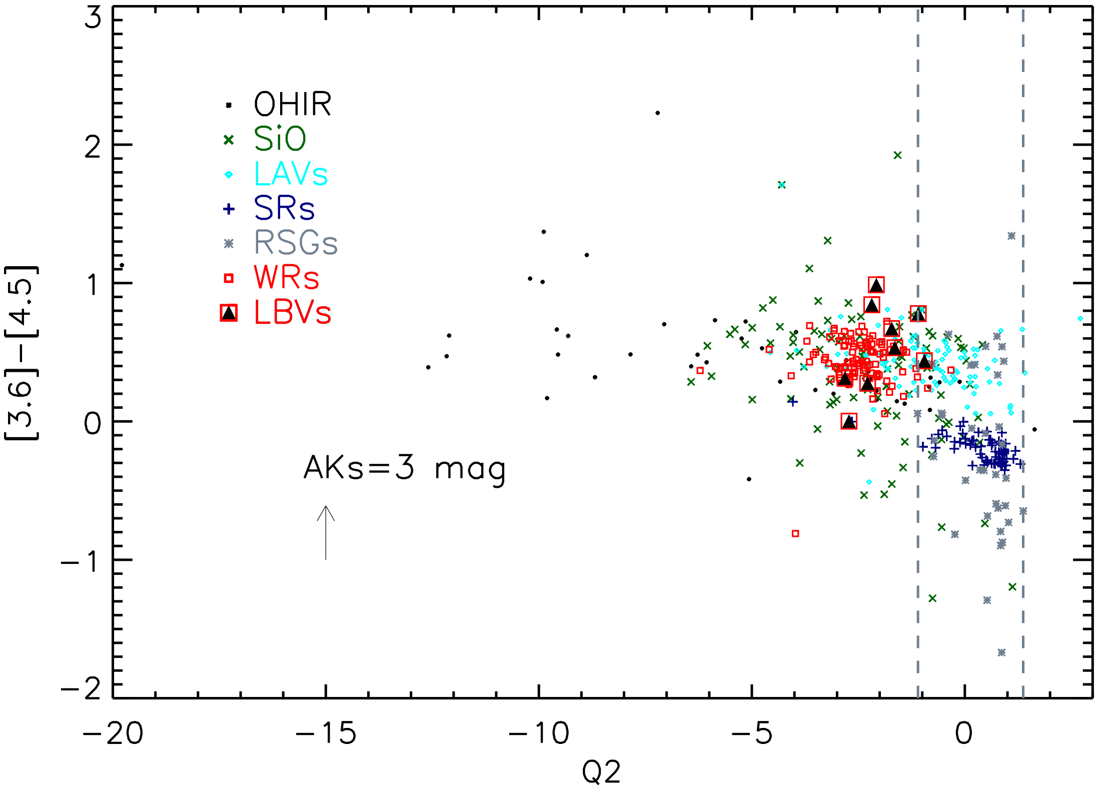

Fig. 5. $Q2$ parameter versus the GLIMPSE [3.6] – [4.5] color. Symbols are as in Fig. 1. The arrow represents the reddening vector following the extinction ratios given by Indebetouw et al. (2005). Dashed vertical lines at $Q2=-1.1$ mag and $Q2=1.37$ mag indicate the region populated by RSG stars. Stars in this range and with $[3.6]-[4.5] < -0.4$ mag are highly probable RSG stars. Typical errors are 0.13 mag in the x-axis and 0.08 mag in the y-axis.

windy hot stars (e.g. WRs). Contamination by other stars can be reduced by taking into account luminosity and distance information.

The $Q2$ values is based on near and mid-infrared data, which are not taken simultaneously. In order to reduce the uncertainty due to non simultaneity, we use information on variability, e.g., flags provided in the MSX catalog, comparison of the 8 μm measurements from GLIMPSE and MSX (e.g. Robitaille et al. 2007), and of the J and K_s measurements from 2MASS and DENIS K_s (e.g. Messineo et al. 2004; Schultheis & Glass 2001).

In the following, we list our new proposed classification steps.

- With available J, H, K_s magnitudes from 2MASS and 8.0μm magnitudes from GLIMPSE or MSX, we calculate the $Q1$ and $Q2$ parameters.
- We classify as late-types those stars located above the relation $Q1 = -0.20\times(K_S-[8.0])+0.34$ mag (see Fig. 4), and we classify as early-type stars those stars below it. This relation applies only to stars with $K_s-[8.0] < 4$ mag.
- To explore the impact of each constraint, we select candidate early-type stars with free-free emission in several manners. We call ”free-1” stars those early-type stars with $Q2 < -1$ mag, and ”free-2” stars with the additional condition $Q2 > 11.25 \times Q1 - 2.38$ mag. We call ”free-3” stars with extra additional conditions, the GLIMPSE criteria specified by Hadfield et al. (2007); Mauerhan et al. (2011). We compare the new criteria with those used by Mauerhan et al. (hereafter, called ”free-MVM11” 2011).
- We select late-type stars with $0.1 < Q1 < 0.5$ mag and $-1.1 < Q2 < 1.5$ as candidate RSGs (cRSG1), or more stringently with $0.1 < Q1 < 0.5$ mag and $+0.5 < Q2 < 1.5$ mag (cRSG2). When using the additional condition $[3.6]-[4.5] < -0.4$ mag, a detection rate of 70% is expected (see Fig. 5). We call this more restricted color selection as cRSG3. We do not consider candidate RSGs with an indication of variability.
- The degeneracy between candidate RSGs and AGB-SRs can be removed by additional information on luminosity, and therefore extinction and distance. We suggest to calculate the total extinction (circumstellar and interstellar) as described in Messineo et al. (2005), and to use the model of Galactic dust distribution by Drimmel et al. (2003) for estimating distances. With bolometric corrections, distances, and extinction estimates, luminosities can be derived.

For each of the samples, we ignored the a priori knowledge on spectral types, and calculated the fractions of retrieved free-free emitters and RSGs, by using the categories defined above. The results of our experiments are listed in Table 4.

The selection of early and late-type stars retrieves 85% of WR stars from van der Hucht (2001), but only 63% of SR stars, and 48% of the OH/IR stars listed by Alard et al. (2001).

The Q2 parameter is a good discriminant for selecting free-free emitters (”free-1”); additional constraints on GLIMPSE colors are needed to reduce contamination by late-type stars (”free-3”). The pre-selection of early and late-type stars allows retrieval of 75% of free-free emitters, but strongly reduces the contamination by AGBs; the number of AGB stars erroneously retrieved as free-free emitters decreases from 33% (”free-1”) to a few percent (”free-3”). For a comparison with Mauerhan et al. (2011), we also use their selection criteria (Fig. 1 in Mauerhan et al. 2011),

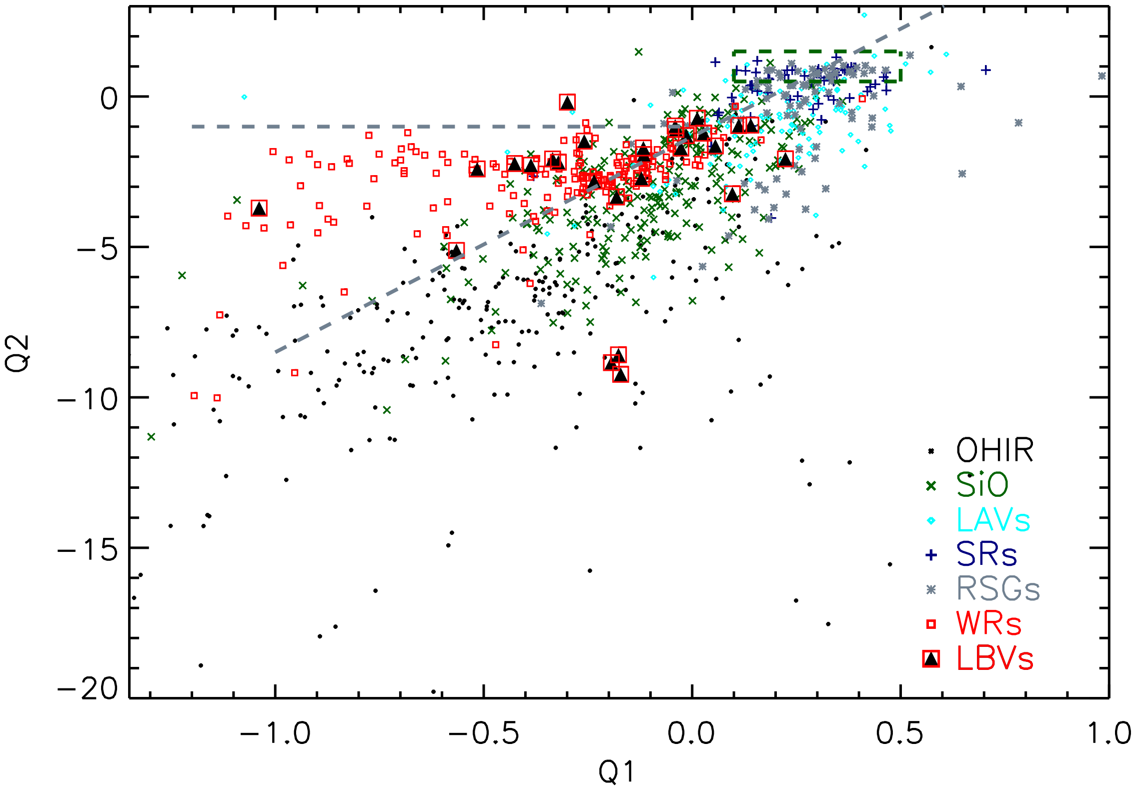

Fig. 6. $Q1$ versus $Q2$ values, which are values independent of interstellar extinction. Plotted symbols are as in Fig. 1. The dashed line ($Q2 = 11.25 \times Q1 - 2.38$ mag) serves as a first approximation to separate early and late-type stars. The dashed box with $0.1 < Q1 < 0.5$ mag and $0.5 < Q2 < 1.5$ mag indicates the selection of candidate RSGs (see text RSG2). WR stars populate the region enclosed by the two lines $Q2 > 11.25 \times Q1 - 2.38$ mag and $Q2 < -1.0$ mag.

Table 4. Fractions of retrieved types.

Type	Early-type	free-1	free-2	free-3	free-MVM11	Late-type	cRSG1	cRSG2	cRSG3
WR all	0.86	0.85	0.85	0.78	0.80	0.14	0.02	0.00	0.00
WR MVM1	0.75	0.73	0.73	0.72	0.73	0.25	0.00	0.00	0.00
WR SFZ1	0.90	0.90	0.90	0.90	0.90	0.10	0.05	0.00	0.00
LBV	0.67	0.67	0.67	0.33	0.44	0.33	0.11	0.00	0.00
RSG	0.11	0.00	0.00	0.00	0.00	0.89	0.72	0.42	0.22
OH/IR	0.52	0.33	0.15	0.00	0.15	0.48	0.04	0.00	0.00
SiO	0.25	0.16	0.16	0.01	0.19	0.75	0.04	0.00	0.00
AGB-LAV	0.03	0.01	0.01	0.01	0.03	0.97	0.36	0.06	0.00
AGB-SR	0.37	0.02	0.02	0.00	0.00	0.63	0.58	0.35	0.00

Notes. For each sample of star, we list the fraction of retrieved early-type (Early-type), three estimates of the fractions of free-free emitters (free-1, free-2, free-3, and free-MVM11), the fraction of retrieved late-type stars (Late-type), and three estimates of RSG stars (cRSG1, cRSG2, cRSG3, and cRSG4). Only stars with counterparts in the three 2MASS and four GLIMPSE bands are considered. For WR stars, we consider the whole sample alltogether (WR all), as well as the newly detected samples by Mauerhan et al. (WR MVM11 2011) and Shara et al. (WR SFZ11 2011). The selection of free-free emitters is applied only to early-type stars; the selection of RSG stars is applied only to late-type stars.

which we label as free-MVM11. The Q1-Q2 based criteria provide a detection efficiency comparable to that by Mauerhan et al. on the whole sample of WRs. These authors applied additional criteria than the color-color criteria by Hadfield et al. (2007), based on the K_s versus J–K_s diagram. We also reclassified separately their sample of 61 WRs, which is composed of more distant and obscured WR stars with our classification scheme, and retrieved 75% of them as early-type stars, and 73% as free-free emitters (free-1).

The selection of a narrow window in the $Q1$ versus $Q2$ plane with the additional limits on GLIMPSE colors allows selecting bonafide RSG stars.

7. Summary and discussion

7.1. Summary

We analyzed 2MASS and GLIMPSE color properties of samples of Galactic evolved stars. Samples of O-rich AGB stars (SRs, Miras, OH/IR stars, and SiO masing stars), RSG stars, WRs, and LBVs were collected from existing literature. Several color-color diagrams were analyzed, aiming to identify the best combination for stellar photometric classifications.

The $J - H$ versus H–K_s diagram, and the J–K_s versus K_s–[8.0] diagram are particular useful. In these planes, the colors of WR stars and mass-losing late type stars deviate from the interstellar reddening vector. WRs have a mid-infrared excess due to their free-free emission. Late-type stars often have mid-infrared excess due to their dusty envelopes. The deviation from the reddening vector in the K_s–[8.0] versus J–K_s plane increases going from SRs to Miras and OH/IR stars, i.e. with increasing mass-loss rates.

The $J - H$ versus H–K_s, and the J–K_s versus K_s–[8.0] diagrams together can be used to discriminate between interstellar and circumstellar reddening, and identify different types of stars with envelopes. Stellar classification is hampered by color overlaps between sources of different types, and scatter due to variability and non-simultaneity of the observations. Special color windows have been identified for locating WR and RSG stars.

We investigated two extinction free parameters, $Q1$ and $Q2$. $Q1$ is a measure of the deviation from the reddening vector in the $J - H$ versus H–K_s plane (Negueruela & Schurch 2007). $Q2$ is a newly defined parameter, which measures the deviation from the reddening vector in the J–K_s versus K_s–[8.0] plane. The $Q1$ and $Q2$ parameters allow for an efficient selection of stars with free-free emission (e.g. WR stars), and candidate RSG stars. Stars with $Q1 < -1.0$ mag and $Q2 > 11.25 \times Q1 - 2.38$ mag are candidate hot massive stars with free-free radiation. A large number ($\sim$ 40%) of Galactic RSGs are found with $0.1 < Q1 < 0.5$ mag, and $-1.1 < Q2 < 1.5$ mag. Selections can be further improved with additional conditions (e.g. with the [3.6] – [4.5] color).

A combination of mid- and near-infrared measurements allows to statistically distinguish between evolved mass-losing stars and early-type stars.

7.2. Selection of free-free emitters

We have found a clear separation between massive stars with free-free emission (e.g. WR stars) and late-type stars in the $Q1$ versus K_s–[8.0] diagram, and in the $Q1$ versus $Q2$ diagram.

A combination of [3.6] – [8.0] versus [3.6] – [4.5] and K_s–[8.0] versus J–K_s diagrams (Figs. 3 and 2) were chosen by Hadfield et al. (2007) to best identify WR stars from other field stars. Recently, Mauerhan et al. (2011) revised the selection of WR stars with additional constrains on the H–K_s versus J–K_s diagram, and K_s versus J–K_s diagram, to obtained a spectroscopic detection rate of 95% in early-type stars, and 20% in WR stars. The criteria suggested by Hadfield et al. (2007) and Mauerhan et al. (2011) depend on interstellar extinction, and suffer some contamination by dust enshrouded AGBs. Our new selection based on $Q1$ and $Q2$ has the advantage of simplicity, based on a single diagram that is independent of interstellar extinction. A fraction of WRs (about 15 %), however, are found in the region of late-type stars, and are missed by our selection of early type stars – among them several WC stars, which are known to have dusty envelopes.

The complex structures of LBV envelopes, which are dusty and often extended, result in a broad range of colors. $Q2$ varies from −2.2 to −0.7 mag and $Q1$ from −0.34 to 0.0 mag. LBVs occupy a broad color spaces, and cannot be identified with photometry of point sources alone.

7.3. Pulsation and stellar colors

A correlation is newly found between pulsation types and GLIMPSE colors. Alvarez et al. (2000) writes: ”Pulsation produces much more extended atmospheres, and in addition dense cool layers may result from the periodic outwards running shocks. In various ways pulsation thus leads to the existence of regions where relatively low temperatures are combined with relatively high densities, conditions that favor the formation of water, and dust.”

For AGBs, we have located a sequence of increasing [3.6] – [8.0] colors with increasing pulsation amplitudes (from SRs to OH/IR stars). The behaviors of the [3.6] – [4.5] color with spectral types is more complex. Generally, SRs and LAVs (without SiO maser) show a nice correlation of increasing [3.6] – [4.5] colors with increasing [3.6] – [8.0] colors, but the subgroup of SiO masing stars appears to be more scattered and to have bluer [3.6] – [4.5] colors. In the Appendix, a few ISO-SWS representative spectra of evolved late-type stars are shown. The increase in [3.6] – [4.5] colors going from SRs to LAVs is due to strong continuum absorption by water in the GLIMPSE 3.6 μm band (Matsuura et al. 2002). In contrast, the bluer color of masing AGB stars is likely due to a combination of stronger water absorption (3.6 μm band), and presence of absorption due to SiO and CO_2 molecules in the 4.5 μm band.

Several parameters, such as luminosity, rotation, turbulence, and metallicity, play an important role in determining the dust chemistry of RSG envelopes. RSG stars with regular pulsation display redder [3.6] – [4.5] color than irregular RSGs, as suggested by existing ISO-SWS spectra (see Appendix). Pulsation appears, therefore, a key parameter for mass-loss rates also in RSG stars. The GLIMPSE [3.6] – [4.5] and [3.6] – [8.0] colors of RSGs correlate with mass-loss rates (see Appendix). RSGs show a broad range of [3.6] – [4.5] colors, and can be bluer than AGB stars. Photometric monitoring of Galactic RSGs, as well as follow-up mid-infrared spectroscopic observations of the 3 μm region, is needed to further explore a correlation between chemistry and pulsation properties in RSGs, as suggested by Fig. 3. The RSGCs share the same location in the Galaxy, and likely have similar metallicity (Davies et al. 2009b), but their RSG members have a large spread in [3.6] – [4.5] colors. This suggests that pulsation affect the mid-infrared properties of RSGs more than metallicity.

7.4. Selection of RSG stars

We confirm that the selection of RSGs based on $Q1$ values adopted by Clark et al. (2009), Negueruela et al. (2010), and Negueruela et al. (2011) (as remarked already in these works) excludes possible dust enshrouded RSG stars, and its strongly contaminated by AGBs (SRs and Miras). Selection of bonafide RSG stars solely based on the $Q1$ parameter is impossible. The $Q1$ parameter remains, however, a valid tool to select clusters with RSGs. RSGs are often found in massive clusters, because of their young ages (< 30 Myr) (e.g. Davies et al. 2007; Figer et al. 2006). Masing AGBs are typically found in isolation (e.g. Messineo et al. 2002; Sevenster 2002; Sjouwerman et al. 1998).

We propose a selection of candidate RSG stars based on a larger set of constraints: the $Q1$ and $Q2$ values, variability information, [3.6] – [4.5] colors, and apparent magnitudes. We can distinguish between interstellar and circumstellar extinction, using the $Q1$ and $Q2$ parameters. First distance estimates can be obtained by assuming an interstellar-extinction versus distance relation (Drimmel et al. 2003); stellar luminosities can, then, be estimated by using adeguate bolometric corrections.

7.5. Final remarks

While our new criteria do not allow classification of all IR bright Galactic stars detected by GLIMPSE or MSX, the number of known WR stars and RSGs can highly be increased. The proposed criteria are particularly useful for studying stellar populations, for which an average extinction and distance can be assumed. They will allow to efficiently detect massive stars in giant HII regions and supernova remnants.

The presented datasets open new possibilities for addressing, and pose questions concerning our understanding of stellar reddening, bolometric corrections, and extinction ratios.

Appendix A: ISO-SWS spectra of late-type stars

Molecular absorption and/or emission and dust features affect the [3.6] – [4.5] and [3.6] – [8.0] colors. In order to understand the observed trend of increasing [3.6] – [4.5] and [3.6] – [8.0] colors of late-type stars with pulsation types, we analysed ISO-SWS spectra (see Fig. .1). From the flux-calibrated ISO-SWS library of Sloan et al. (2003), we selected spectra of stars with known spectral types and variabilities: AGB-Miras, AGB-SRs, and OH/IR stars, and RSGs.

Water, SiO, CO_2, and CO absorption may be present in the 3.0 to 5.0 μm spectral region of late-type stars (Cami 2002; Matsuura et al. 2002; Sylvester et al. 1999). ISO-SWS spectra of RSGs and AGB-SRs are remarkably different from those of AGB Miras (see Fig. .1). Typically RSGs and AGB-SRs do not have strong molecular signatures in between 3 and 4 μm, and display a decreasing flux in this region (GLIMPSE 3.6 μm). AGB-Miras are dominated by water, SiO, CO_2, and CO absorption, and the resulting spectral flux between 3 and 4 μm can have a positive slope. This is attributed to a different ”MOLspheres”, layers of molecular material in an extended atmosphere (Miras), where water is the main source of opacity (Matsuura et al. 2002; Tsuji et al. 1997; Verhoelst et al. 2009). The strength of water absorption varies with stellar pulsation phase (Matsuura et al. 2002).

Verhoelst et al. (2009) explains the continuum shape of RSGs in the 2.5-3 μm regions with an extra dust component (metallic Fe, amorphous C, or O-rich micron-sized grains) or with chromospheric emission. The similarity of the continuum of AGB SRs and RSG stars in the 2.5 and 3 μm region suggests that the attribution of extra continuum emission to free-free radiation from chromospheric activities is less likely. Regularly pulsating RSGs have larger mass-loss (as suggested by the strength of the silicate emission at 9.7 μm) than RSGs with irregular pulsations (Fig. .1).

The ISO-SWS flux densities at the effective wavelength of the GLIMPSE filters were measured, and flux densities were converted into magnitudes using the GLIMPSE zero-points. The synthetic [3.6]−[4.5] versus [3.6]−[8.0] diagram is shown in Fig. .2, and well reproduces the sequence of increasing [3.6] – [4.5] with [3.6]−[8.0] colors. A clear sequence of redder colors is seen in AGB stars, going from SRs, to Miras and OH/IR stars. An increase in the [3.6]−[8.0] color is mostly due to an increase of silicate emission at 9.7 μm, which for optically thin envelopes well correlates with mass-loss. Their [3.6] – [4.5] colors are redder than those of AGB SR stars (Figs. .1), because in the spectra of Miras there is strong water absorption. RSGs and AGB SR stars have weaker water absorption than AGB Miras. Yang & Jiang (2011) suggest that RSGs have bluer [3.6] – [4.5] due to a continuum depression around 4.5 μm by CO bands. RSG-SR stars have redder [3.6] – [4.5] colors than RSGs with irregular pulsations. Only weak water absorption is seen in some variable RSG stars.

In Fig. .3, we plot our synthetic GLIMPSE colors of RSG stars versus mass-loss rates, as inferred by Verhoelst et al. (2009). Both [3.6] – [4.5] and [3.6] – [8.0] colors correlate with mass-loss rates. The correlation of mass loss with the [3.6]−[8.0] is explained by the increasing silicate strength at 9.7 μm. The correlation of mass loss with [3.6] – [4.5] color can be due to CO at 4.3 μm, and/or to the existence of an extra source of opacity (dust component), as suggested by Verhoelst et al. (2009).

Acknowledgements. This publication makes use of data products from the Two Micron All Sky Survey, which is a joint project of the University of Massachusetts and the Infrared Processing and Analysis Center/California Institute of Technology, funded by the National Aeronautics and Space Administration and the National Science Foundation. This work is based [in part] on observations made with the Spitzer Space Telescope, which is operated by the Jet Propulsion Laboratory, California Institute of Technology under a contract with NASA. The DENIS project was supported, in France by the Institut National des Sciences de l’Univers, the Education Ministry and the Centre National de la Recherche Scientifique, in Germany by the State of Baden-Wrtemberg, in Spain by the DGICYT, in Italy by the Consiglio Nazionale delle Ricerche, in Austria by the Fonds zur Frderung der wissenschaftlichen Forschung and the Bundesministerium fuer Wissenschaft und Forschung. This research made use of data products from the Midcourse Space Experiment, the processing of which was funded by the Ballistic Missile Defence Organization with additional support from the NASA office of Space Science. This research has made use of the SIMBAD data base, operated at CDS, Strasbourg, France. This work was funded by the ERC Advanced Investigator Grant GLOSTAR (247078). MM thanks Jon Mauerhan for sending her the ”broad” color criterion for WR stars. MM is grateful to Frank Bertoldi, Don Figer, Vasilii Gvaramadze, Peter-Rolf Kudritzki, and Maria Massi for stimulating discussions on massive stars. We thank the referee Guandanlini Roald for his careful reading of our manuscript.

References

Abraham, Z., Falceta-Gonçalves, D., Dominici, T., Caproni, A., & Jatenco-Pereira, V. 2005, MNRAS, 364, 922
Alard, C., Blommaert, J. A. D. L., Cesarsky, C., et al. 2001, ApJ, 552, 289
Alcock, C., Allsman, R. A., Alves, D. R., et al. 1999, PASP, 111, 1539
Alvarez, R., Lançon, A., Plez, B., & Wood, P. R. 2000, A&A, 353, 322
Barniske, A., Oskinova, L. M., & Hamann, W. 2008, A&A, 486, 971
Benjamin, R. A., Churchwell, E., Babler, B. L., et al. 2003, PASP, 115, 953
Bernabei, S. & Polcaro, V. F. 2001, A&A, 366, 817
Bibby, J. L., Crowther, P. A., Furness, J. P., & Clark, J. S. 2008, MNRAS, 386, L23
Blum, R. D., Ramírez, S. V., Sellgren, K., & Olsen, K. 2003, ApJ, 597, 323
Bonanos, A. Z., Lennon, D. J., Köhlinger, F., et al. 2010, AJ, 140, 416
Bressan, A. G., Chiosi, C., & Bertelli, G. 1984, A&A, 130, 279
Buchanan, C. L., Kastner, J. H., Forrest, W. J., et al. 2006, AJ, 132, 1890
Buchanan, C. L., Kastner, J. H., Hrivnak, B. J., & Sahai, R. 2009, AJ, 138, 1597
Cami, J. 2002, PhD thesis, University of Amsterdam
Caron, G., Moffat, A. F. J., St-Louis, N., Wade, G. A., & Lester, J. B. 2003, AJ, 126, 1415
Churchwell, E., Babler, B. L., Meade, M. R., et al. 2009, PASP, 121, 213
Clark, J. S., Egan, M. P., Crowther, P. A., et al. 2003, A&A, 412, 185
Clark, J. S., Larionov, V. M., & Arkharov, A. 2005, A&A, 435, 239
Clark, J. S., Negueruela, I., Davies, B., et al. 2009, A&A, 498, 109
Cohen, M., Kuhi, L. V., & Barlow, M. J. 1975, A&A, 40, 291
Comerón, F., Torra, J., Chiappini, C., et al. 2004, A&A, 425, 489
Conti, P. S., Hanson, M. M., Morris, P. W., Willis, A. J., & Fossey, S. J. 1995, ApJ, 445, L35
Cutri, R. M., Skrutskie, M. F., van Dyk, S., et al. 2003, 2MASS All Sky Catalog of point sources.
Davies, B., Figer, D. F., Kudritzki, R., et al. 2007, ApJ, 671, 781
Davies, B., Figer, D. F., Kudritzki, R., et al. 2009a, ApJ, 707, 844
Davies, B., Figer, D. F., Law, C. J., et al. 2008, ApJ, 676, 1016
Davies, B., Origlia, L., Kudritzki, R., et al. 2009b, ApJ, 696, 2014
Deguchi, S., Fujii, T., Glass, I. S., et al. 2004, PASJ, 56, 765
Drimmel, R., Cabrera-Lavers, A., & López-Corredoira, M. 2003, A&A, 409, 205
Egan, M. P., Price, S. D., Kraemer, K. E., et al. 2003, VizieR Online Data Catalog, 5114, 0
Eggenberger, P., Meynet, G., & Maeder, A. 2002, A&A, 386, 576

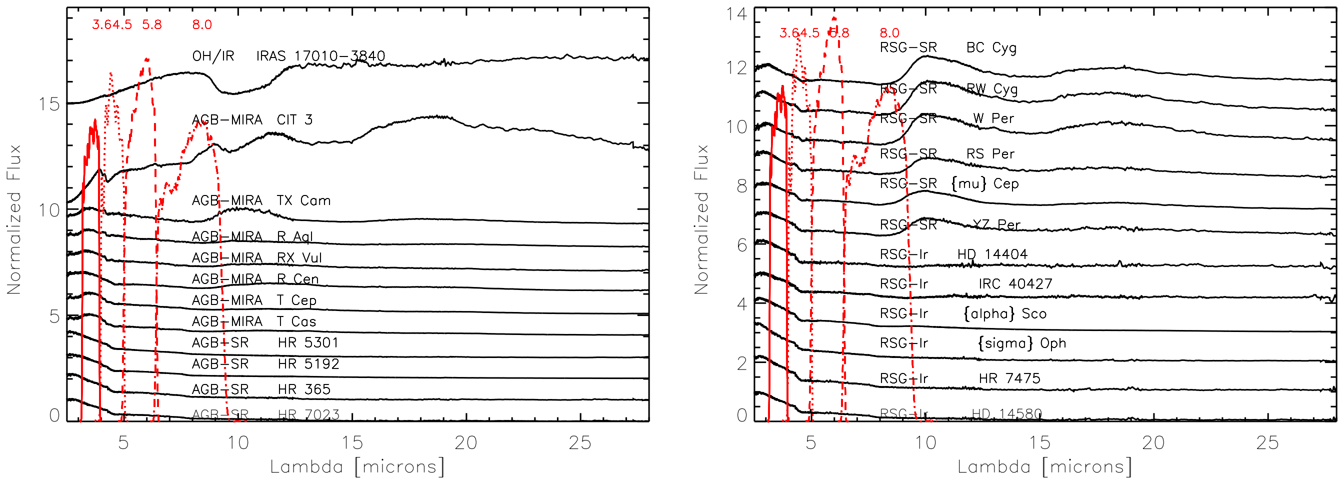

Fig. .1. Left: A representative samples of ISO-SWS spectra of AGB stars. Over-plotted transmission curves of the four SPITZER/IRAC filters. Right: A representative samples of ISO-SWS spectra of RSG stars. Over-plotted transmission curves of the four SPITZER/IRAC filters.

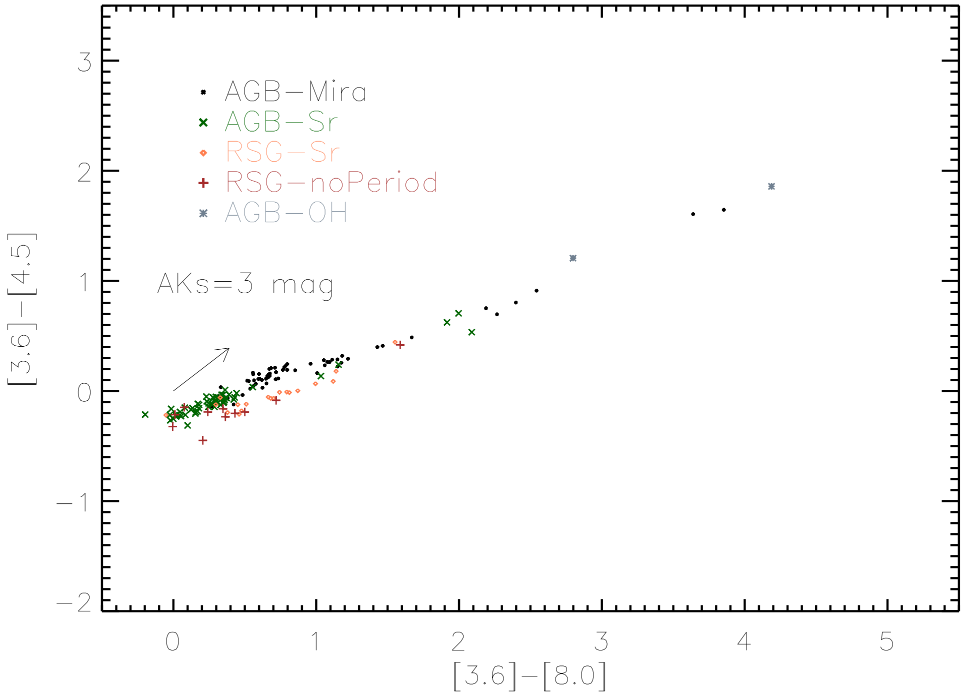

Fig. .2. Synthetic GLIMPSE [3.6]−[8.0] versus [3.6]−[4.5] diagram of evolved late-type stars observed with ISO-SWS (Sloan et al. 2003). AGB-Miras are shown with black dots, AGB-SR with crosses, RSG-SR with diamonds, RSG irregular with plus signs, and OH/IR stars with starred symbols. The arrow indicates the direction of the reddening vector following the extinction ratios derived by Indebetouw et al. (2005).

Epchtein, N., Deul, E., Derriere, S., et al. 1999, VizieR Online Data Catalog, 1, 2002
Fazio, G. G., Hora, J. L., Allen, L. E., et al. 2004, ApJS, 154, 10
Felli, M. & Panagia, N. 1981, A&A, 102, 424
Figer, D. F., MacKenty, J. W., Robberto, M., et al. 2006, ApJ, 643, 1166
Figer, D. F., McLean, I. S., & Morris, M. 1999, ApJ, 514, 202
Figer, D. F., McLean, I. S., & Najarro, F. 1997, ApJ, 486, 420
Fritz, T. K., Gillessen, S., Dodds-Eden, K., et al. 2011, ApJ, 737, 73
Frogel, J. A. & Whitford, A. E. 1987, ApJ, 320, 199
Gehrz, R. 1989, in IAU Symposium, Vol. 135, Interstellar Dust, ed. L. J. Allamandola & A. G. G. M. Tielens, 445
Georgelin, Y. M. & Georgelin, Y. P. 1976, A&A, 49, 57
Glass, I. S., Matsumoto, S., Carter, B. S., & Sekiguchi, K. 2001, MNRAS, 321, 77
Groenewegen, M. A. T. & de Jong, T. 1993, A&A, 267, 410
Gvaramadze, V. V., Kniazev, A. Y., Fabrika, S., et al. 2010, MNRAS, 405, 520
Habing, H. J. 1996, A&A Rev., 7, 97
Habing, H. J. & Olofsson, H., eds. 2003, Asymptotic giant branch stars
Habing, H. J., Sevenster, M. N., Messineo, M., van de Ven, G., & Kuijken, K. 2006, A&A, 458, 151
Hadfield, L. J., van Dyk, S. D., Morris, P. W., et al. 2007, MNRAS, 376, 248
Harwit, M., Malfait, K., Decin, L., et al. 2001, ApJ, 557, 844
Homeier, N. L., Blum, R. D., Pasquali, A., Conti, P. S., & Damineli, A. 2003, A&A, 408, 153
Imai, H., Deguchi, S., Fujii, T., et al. 2002, PASJ, 54, L19
Indebetouw, R., Mathis, J. S., Babler, B. L., et al. 2005, ApJ, 619, 931
Josselin, E., Blommaert, J. A. D. L., Groenewegen, M. A. T., Omont, A., & Li, F. L. 2000, A&A, 357, 225
Kemper, F., Waters, L. B. F. M., de Koter, A., & Tielens, A. G. G. M. 2001, A&A, 369, 132

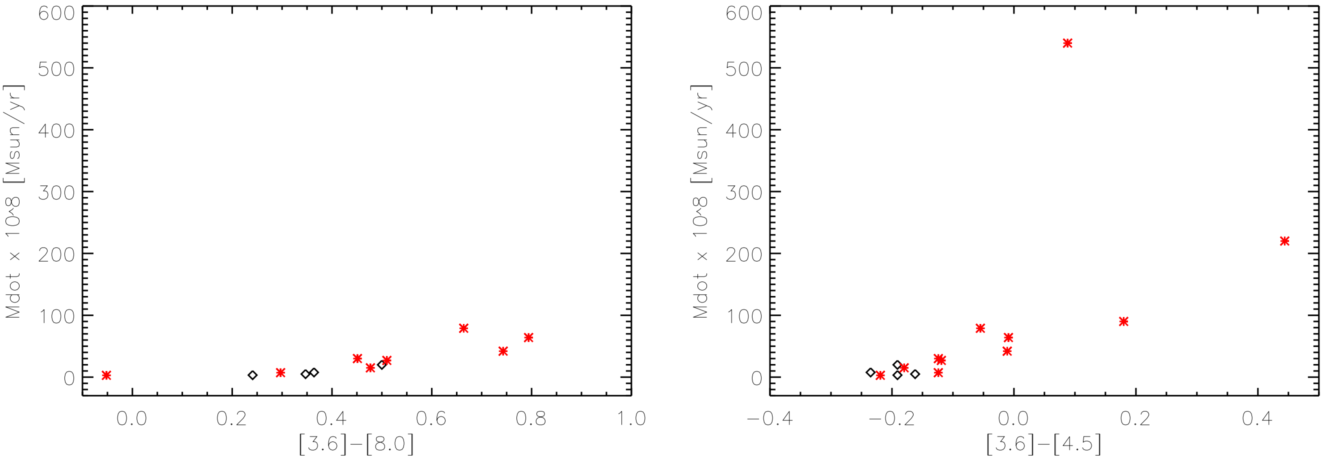

Fig. .3. Right: Synthetic [3.6] – [4.5] of RSG stars versus mass-loss rates. Magnitudes are obtained from ISO-SWS spectra (Sloan et al. 2003), and mass-loss rates are given by Verhoelst et al. (2009). Starred symbols are RSG stars with periodic pulsations (SR), while diamonds are irregular RSG stars. Left: Synthetic [3.6] – [8.0] of RSG stars modeled by Verhoelst et al. (2009) versus their inferred mass-loss rates. Starred symbols are RSG stars with periodic pulsations (SR), while diamonds are irregular RSG stars.

Koornneef, J. 1983, A&A, 128, 84
Lamers, H. J. G. L. M., Nota, A., Panagia, N., Smith, L. J., & Langer, N. 2001, ApJ, 551, 764
Landini, M., Natta, A., Salinari, P., Oliva, E., & Moorwood, A. F. M. 1984, A&A, 134, 284
Levesque, E. M., Massey, P., Olsen, K. A. G., et al. 2005, ApJ, 628, 973
Lucas, P. W., Hoare, M. G., Longmore, A., et al. 2008, MNRAS, 391, 136
Martins, F., Genzel, R., Hillier, D. J., et al. 2007, A&A, 468, 233
Matsuura, M., Yamamura, I., Cami, J., Onaka, T., & Murakami, H. 2002, A&A, 383, 972
Mauerhan, J. C., Morris, M. R., Cotera, A., et al. 2010, ApJ, 713, L33
Mauerhan, J. C., Van Dyk, S. D., & Morris, P. W. 2011, AJ, 142, 40
Mengel, S. & Tacconi-Garman, L. E. 2007, A&A, 466, 151
Mermilliod, J. C., Mayor, M., & Udry, S. 2008, A&A, 485, 303
Messineo, M. 2004, PhD thesis, Leiden Observatory, Leiden University, P.O. Box 9513, 2300 RA Leiden, The Netherlands
Messineo, M., Davies, B., Figer, D. F., et al. 2011, ApJ, 733, 41
Messineo, M., Davies, B., Ivanov, V. D., et al. 2009, ApJ, 697, 701
Messineo, M., Figer, D. F., Davies, B., et al. 2010, ApJ, 708, 1241
Messineo, M., Habing, H. J., Menten, K. M., Omont, A., & Sjouwerman, L. O. 2004, A&A, 418, 103
Messineo, M., Habing, H. J., Menten, K. M., et al. 2005, A&A, 435, 575
Messineo, M., Habing, H. J., Sjouwerman, L. O., Omont, A., & Menten, K. M. 2002, A&A, 393, 115
Minniti, D., Lucas, P. W., Emerson, J. P., et al. 2010, New A, 15, 433
Negueruela, I., González-Fernández, C., Marco, A., & Clark, J. S. 2011, A&A, 528, A59
Negueruela, I., González-Fernández, C., Marco, A., Clark, J. S., & Martínez-Núñez, S. 2010, A&A, 513, A74
Negueruela, I. & Schurch, M. P. E. 2007, A&A, 461, 631
Nishiyama, S., Nagata, T., Kusakabe, N., et al. 2006, ApJ, 638, 839
Norci, L., Polcaro, V. F., Viotti, R. F., & Rossi, C. 2002, Rev. Mexicana Astron. Astrofis., 38, 83
Nota, A., Livio, M., Clampin, M., & Schulte-Ladbeck, R. 1995, ApJ, 448, 788
Olivier, E. A., Whitelock, P., & Marang, F. 2001, MNRAS, 326, 490
Ortiz, R., Blommaert, J. A. D. L., Copet, E., et al. 2002, A&A, 388, 279
Pasquali, A., Nota, A., Smith, L. J., et al. 2002, AJ, 124, 1625
Peeters, E., Hony, S., Van Kerckhoven, C., et al. 2002, A&A, 390, 1089
Pierce, M. J., Jurcevic, J. S., & Crabtree, D. 2000, MNRAS, 313, 271
Price, S. D., Egan, M. P., Carey, S. J., Mizuno, D. R., & Kuchar, T. A. 2001, AJ, 121, 2819
Rieke, G. H., Lebofsky, M. J., & Low, F. J. 1985, AJ, 90, 900
Robitaille, T. P., Cohen, M., Whitney, B. A., et al. 2007, AJ, 134, 2099
Schuller, F., Ganesh, S., Messineo, M., et al. 2003, A&A, 403, 955
Schultheis, M. & Glass, I. S. 2001, MNRAS, 327, 1193
Sevenster, M. N. 1999, MNRAS, 310, 629
Sevenster, M. N. 2002, AJ, 123, 2772
Shara, M. M., Faherty, J. K., Zurek, D., et al. 2011, ArXiv e-prints
Sjouwerman, L. O., Capen, S. M., & Claussen, M. J. 2009, ApJ, 705, 1554
Sjouwerman, L. O., van Langevelde, H. J., Winnberg, A., & Habing, H. J. 1998, A&AS, 128, 35
Skiff, B. A. 2010, VizieR Online Data Catalog, 1, 2023
Sloan, G. C., Kraemer, K. E., Price, S. D., & Shipman, R. F. 2003, ApJS, 147, 379
Smith, N., Vink, J. S., & de Koter, A. 2004, ApJ, 615, 475
Speck, A. K., Barlow, M. J., Sylvester, R. J., & Hofmeister, A. M. 2000, A&AS, 146, 437
Spitzer Science, C. 2009, VizieR Online Data Catalog, 2293, 0
Stead, J. J. & Hoare, M. G. 2009, MNRAS, 400, 731
Sylvester, R. J., Kemper, F., Barlow, M. J., et al. 1999, A&A, 352, 587
The, C. D. 2005, VizieR Online Data Catalog, 2263, 0
Tsuji, T., Ohnaka, K., Aoki, W., & Yamamura, I. 1997, A&A, 320, L1
Umana, G., Buemi, C. S., Trigilio, C., Leto, P., & Hora, J. L. 2010, ApJ, 718, 1036
van der Hucht, K. A. 2001, VizieR Online Data Catalog, 3215, 0
van der Veen, W. E. C. J. & Habing, H. J. 1988, A&A, 194, 125
van Loon, J. T., Gilmore, G. F., Omont, A., et al. 2003, MNRAS, 338, 857
Vauterin, P. & Dejonghe, H. 1998, ApJ, 500, 233
Verheyen, L., Menten, K. M., & Messineo, M. 2011, A&A to be submitted
Verhoelst, T., van der Zypen, N., Hony, S., et al. 2009, A&A, 498, 127
Waters, L. B. F. M. 2010, in Astronomical Society of the Pacific Conference Series, Vol. 425, Hot and Cool: Bridging Gaps in Massive Star Evolution, ed. C. Leitherer, P. Bennett, P. Morris, & J. van Loon, 267
Whitelock, P. & Feast, M. 1994, Ap&SS, 217, 153
Whitelock, P., Marang, F., & Feast, M. 2000, MNRAS, 319, 728
Whitelock, P. A., Feast, M. W., van Loon, J. T., & Zijlstra, A. A. 2003, MNRAS, 342, 86
Williams, P. M., van der Hucht, K. A., Kidger, M. R., Geballe, T. R., & Bouchet, P. 1994, MNRAS, 266, 247
Wright, A. E. & Barlow, M. J. 1975, MNRAS, 170, 41
Yang, M. & Jiang, B. W. 2011, ApJ, 727, 53
Zacharias, N., Monet, D. G., Levine, S. E., et al. 2004, in Bulletin of the American Astronomical Society, Vol. 36, American Astronomical Society Meeting Abstracts, 1418